

# DGM Seminar "Nano-scale Materials: Characterization-Techniques and Applications"

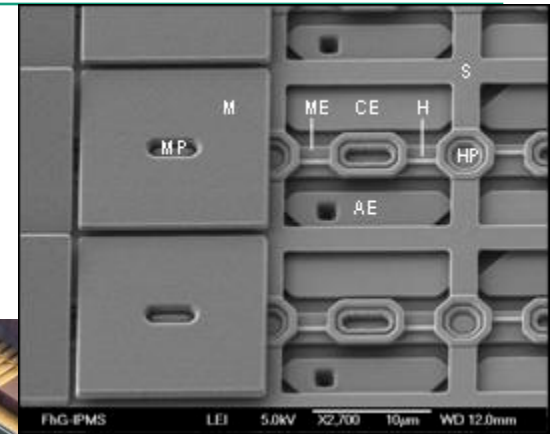
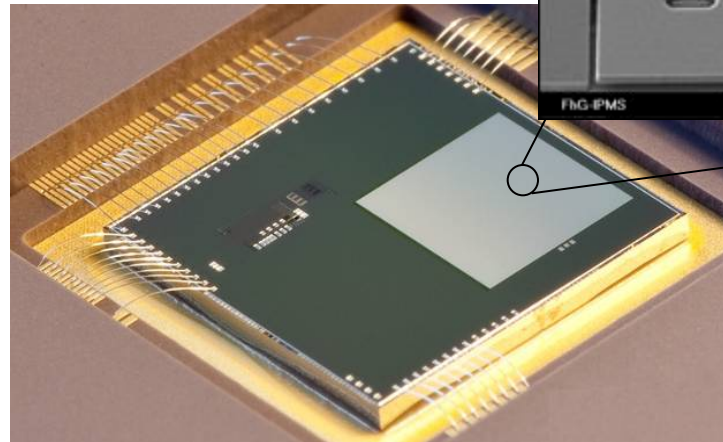
## Thin film analysis: Optical analysis and metrology, X-ray reflectometry

Jan-Uwe Schmidt, Jörg Heber

Fraunhofer Institute for Photonic Microsystems



© J.A. Woolam Co., Inc.



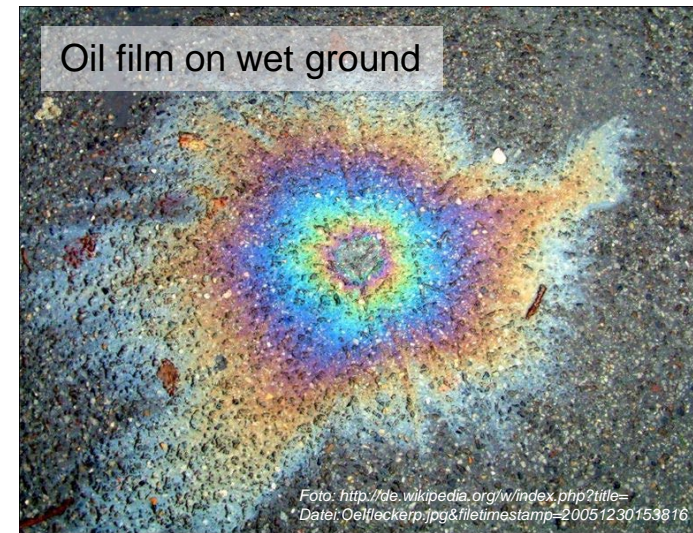
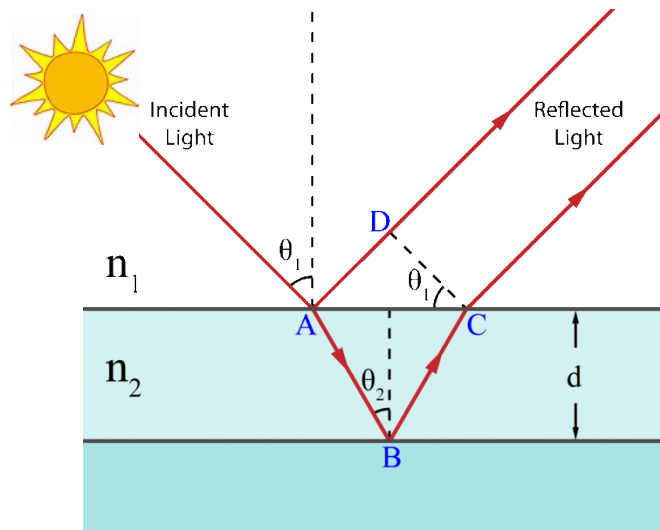
Micromirror array

# Introduction: Light acting as a non-destructive probe

Light waves reflected from interfaces of a thin film interfere.

The reflected intensity depends on wavelength and angle of incidence.

The resulting interference colors carry information on film thickness.



# Aim of this talk

To introduce three test methods using light as a non-destructive probe:

Technique	Measured Quantity
<b>Ellipsometry</b>	<b>Change in polarization</b> of light reflected / transmitted by a planar sample
<b>X-ray reflectometry</b>	<b>Reflectivity</b> (vs. angle of incidence or energy) of smooth planar samples for x-rays
<b>Interferometry</b>	<b>Change in phase</b> of light reflected at a non-planar surface

# Outline

- Ellipsometry
- X-Ray reflectometry
- White light interferometry
- Application to diffractive MEMS

# ELLIPSOMETRY

- Basics
- Measurement principle
- Dispersion models
- Instrumentation
- Applications



© J.A. Woollam Co., Inc.

# Light: Electromagnetic plane wave

Maxwell Eqns. → Wave equations in uniform isotropic source-free medium:

$$\left( \nabla^2 - \mu\varepsilon \frac{\partial^2}{\partial t^2} - \mu\sigma \frac{\partial}{\partial t} \right) \varphi = -\cancel{\rho/\varepsilon}^0$$

$$\left( \nabla^2 - \mu\varepsilon \frac{\partial^2}{\partial t^2} - \mu\sigma \frac{\partial}{\partial t} \right) \vec{A} = -\cancel{\mu\vec{J}}^0$$

Permeability   Permittivity   Conductivity   Scalar potential   Charge density   Vector potential   Current density

Assumption of harmonic time dependence leads to a special solution:  
coupled electro-magnetic transverse plane waves.

Example: Planar wave with field oscillating along x propagating along z.

$$E_x(z, t) = A_x \cos\left( -\frac{2\pi}{\lambda} (z - vt) + \delta_x \right)$$

Amplitude   Wavelength   Phase velocity in medium   Arbitrary phase

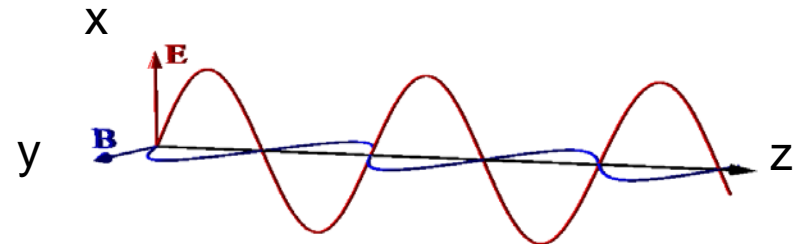
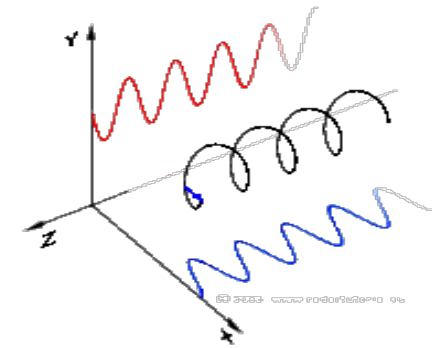


Image: <http://www.kristoflodewijks.be/wp-content/uploads/2013/02/EMwave.gif>

# Polarization of light

monochromatic plane wave traveling in + z direction

$$\vec{E}(\vec{r}, t) = \begin{pmatrix} E_x \\ E_y \\ 0 \end{pmatrix} = \begin{pmatrix} A_x \cos(\omega \cdot t - \vec{k} \cdot \vec{r} + \delta_x) \\ A_y \cos(\omega \cdot t - \vec{k} \cdot \vec{r} + \delta_y) \\ 0 \end{pmatrix}$$



States of polarization:

**Special case: Linear Polarization**

x,y partial waves have phase lag  $\delta = \delta_y - \delta_x$  of  $\delta = \pm a \cdot \pi$ ,  $a = \{0, 1, 2, \dots\}$

$$E_x = \pm \frac{A_x}{A_y} E_y$$

**Special case: Circular Polarization**

Phase lag  $\delta = \pi/2 \pm a \cdot \pi$ ,  $a = \{0, 1, 2, \dots\}$   
Amplitudes:  $A_x = A = \pm A_y$ ,  $A > 0$

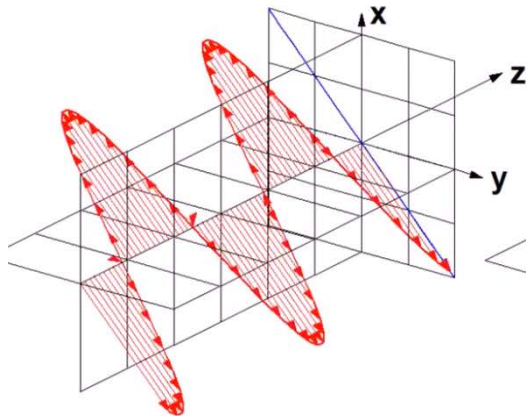
$$E_x^2 + E_y^2 = A^2$$

**General case: Elliptical Polarization**

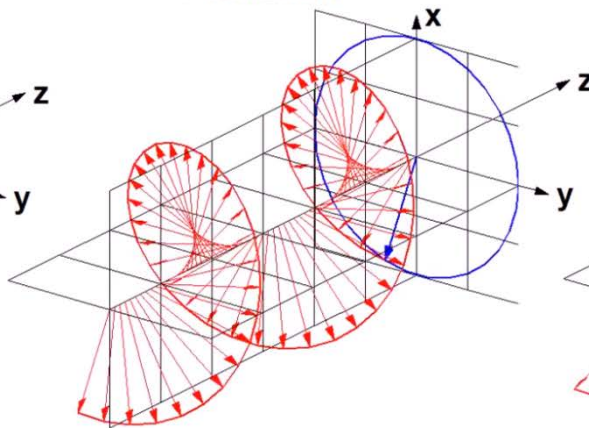
x,y partial waves have arbitrary phase lag  $\delta$  and arbitrary amplitudes  $A_x, A_y$ .

$$\frac{E_x^2}{A_x^2} + \frac{E_y^2}{A_y^2} - 2 \frac{E_x E_y}{A_x A_y} \cos(\delta) + \cos^2(\delta) = 1$$

Linear Polarization



Circular (Right Hand) Polarization



Elliptical (Right Hand) Polarization

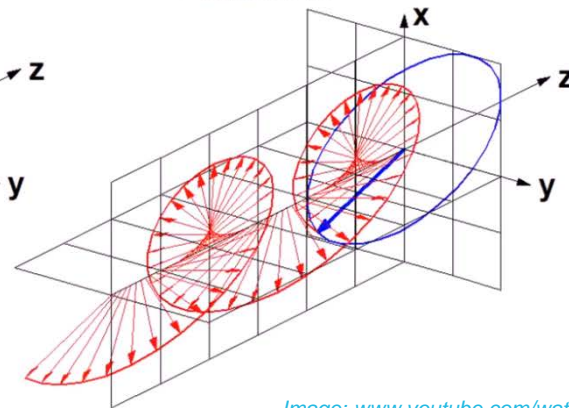
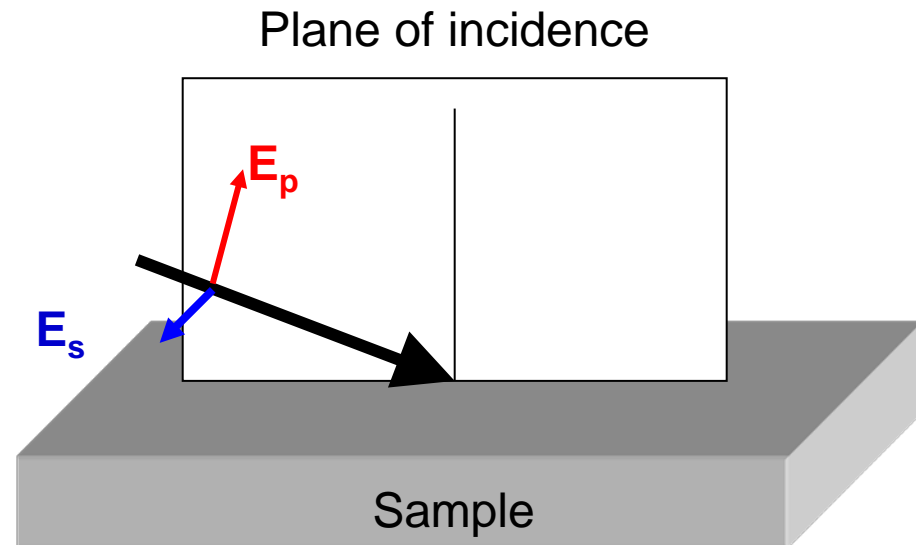


Image: [www.youtube.com/watch?v=Q0qrU4nprB0](http://www.youtube.com/watch?v=Q0qrU4nprB0)

# Polarization of light – „s“ and „p“ polarization

- When considering a plane wave incident on an interface, it is favourable to decompose it into two orthogonal waves polarized linearly perpendicular (s) and parallel (p) to the plane of incidence respectively.

$$\vec{E}(\vec{r}, t) = \begin{bmatrix} E_p \\ E_s \end{bmatrix} = \begin{bmatrix} A_p \cos(\omega \cdot t - \vec{k} \cdot \vec{r} + \delta_p) \\ A_s \cos(\omega \cdot t - \vec{k} \cdot \vec{r} + \delta_s) \end{bmatrix}$$





# Reflection / transmission by a single interface

Considering Maxwell's equations and boundary conditions at interfaces (continuity of  $E_{||}$ ,  $B_{\perp}$ ,  $D_{\perp}$ ,  $H_{||}$ ) an equation for reflection and transmission coefficients for p and s waves can be derived.

## Fresnel equations for reflection / transmission at a single interface

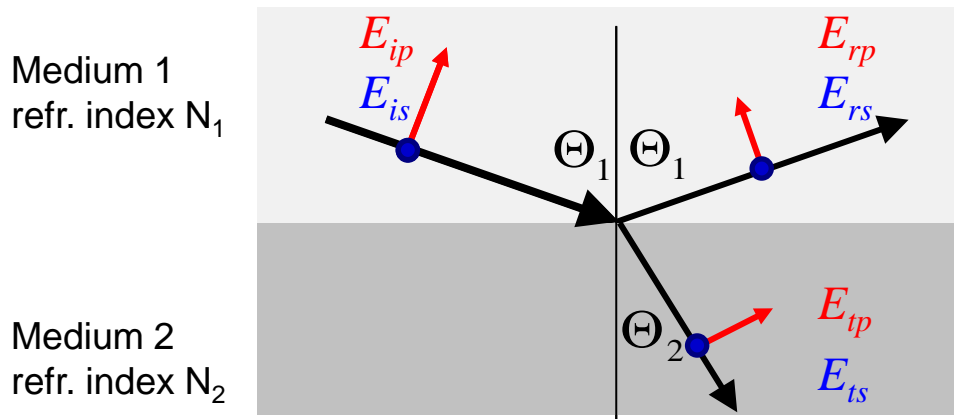
$$t_{12p} = \frac{E_{tp}}{E_{ip}} = \frac{2N_1 \cos \Theta_1}{N_2 \cos \Theta_1 + N_1 \cos \Theta_2}$$

$$r_{12p} = \frac{E_{rp}}{E_{ip}} = \frac{N_2 \cos \Theta_1 - N_1 \cos \Theta_2}{N_2 \cos \Theta_1 + N_1 \cos \Theta_2}$$

$$t_{12s} = \frac{E_{ts}}{E_{is}} = \frac{2N_1 \cos \Theta_1}{N_1 \cos \Theta_1 + N_2 \cos \Theta_2}$$

$$r_{12s} = \frac{E_{rs}}{E_{is}} = \frac{N_1 \cos \Theta_1 - N_2 \cos \Theta_2}{N_1 \cos \Theta_1 + N_2 \cos \Theta_2}$$

$t_{12p}$ ,  $t_{12s}$ ,  $r_{12p}$ ,  $r_{12s}$  are the Fresnel amplitude transmission and reflection coefficients for p and s waves for a single interface respectively.



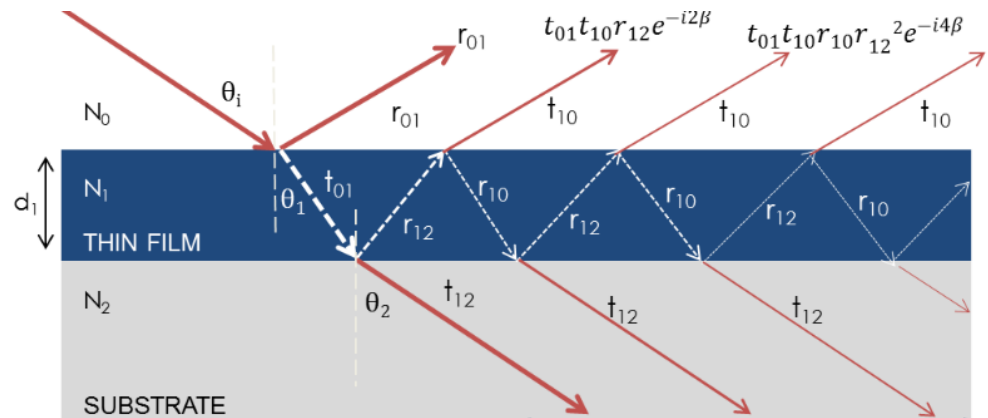
# Reflection of single film on substrate

- For multiple interfaces, multiple reflections must be considered.
- The **overall complex amplitude reflection coefficients** are called  **$R_s$  and  $R_p$** .
- The case single film on surface has an analytical solution\*:

$$R_p = \frac{E_{rp}}{E_{ip}} = \frac{r_{01p} + r_{12p} \exp(-i2\beta)}{1 + r_{01p} r_{12p} \exp(-i2\beta)}$$

$$R_s = \frac{E_{rs}}{E_{is}} = \frac{r_{01s} + r_{12s} \exp(-i2\beta)}{1 + r_{01s} r_{12s} \exp(-i2\beta)}$$

$$\beta = 2\pi \left( \frac{d_1}{\lambda} \right) N_1 \cos(\theta_i)$$



- Higher multilayer systems are solved numerically using recursive algorithms.

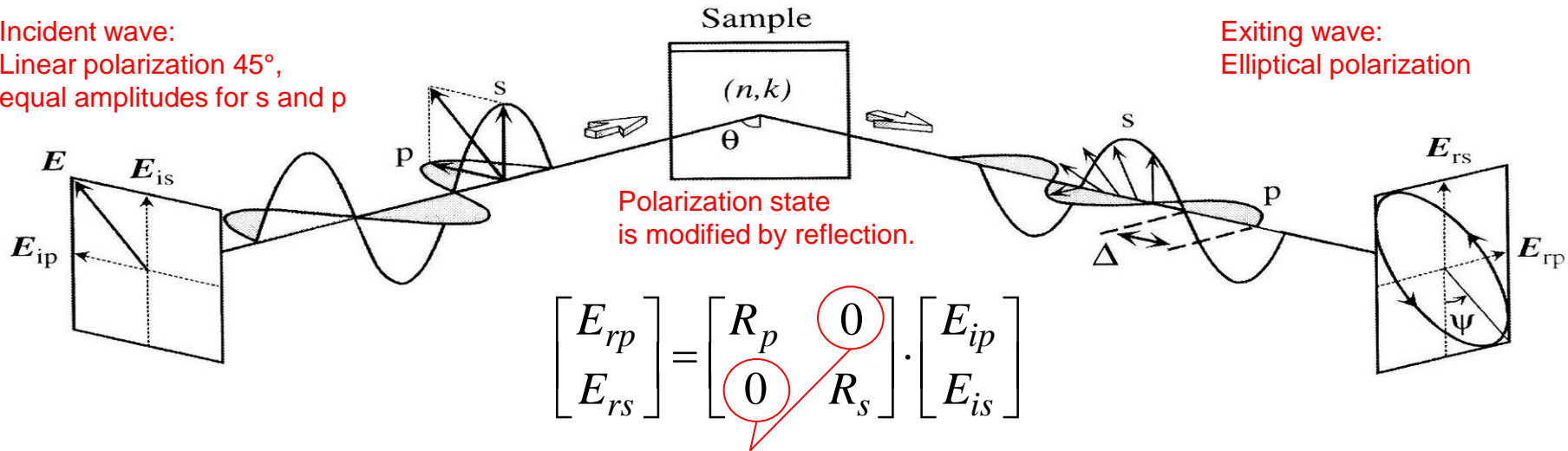
Image:  
Derivation:

<https://www.jawollam.com/resources/ellipsometry-tutorial/interaction-of-light-and-materials>  
W.N. Hansen J. Opt. Soc. Of America, Vol 58, Nr. 3, pp. 380-390 (1968)

# Measurement principle of ellipsometry

Image Source:  
Hiroyuki Fujiwara:  
"Spectroscopic ellipsometry : principles and applications."  
Wiley 2007  
DOI: 10.1002/9780470060193

Incident wave:  
Linear polarization 45°,  
equal amplitudes for s and p



Here isotropic materials (cubic symmetry, amorphous) are assumed. s and p waves do not mix upon reflection.

In case of optical anisotropy off-diagonal elements are non-zero, i.e.  $E_{ip}$  influences  $E_{rs}$ . → Covered by "generalized ellipsometry", not presented here.

- **Ellipsometry measures the change in polarization** in terms of  $\Delta$ , the change in phase lag between s and p waves, and  $\tan \Psi$ , the ratio of amplitude diminutions.

$$\Delta = (\delta_{rp} - \delta_{rs}) - (\delta_{ip} - \delta_{is})$$

$$\tan \Psi = \frac{|E_{rp}| / |E_{ip}|}{|E_{rs}| / |E_{is}|}$$

$$R_p = |E_{rp}| / |E_{ip}| \cdot e^{i(\delta_{rp} - \delta_{ip})}$$

$$R_s = |E_{rs}| / |E_{is}| \cdot e^{i(\delta_{rs} - \delta_{is})}$$

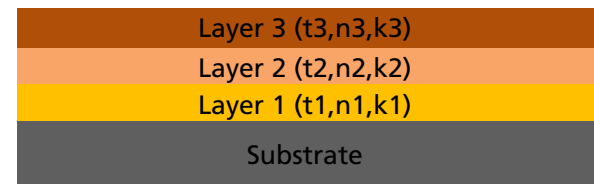
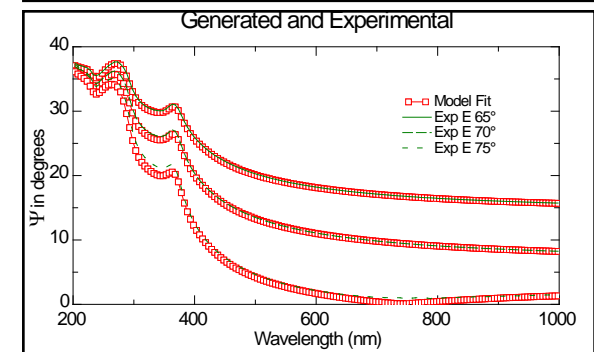
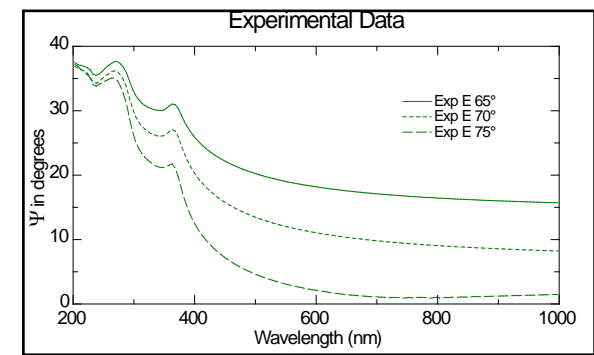
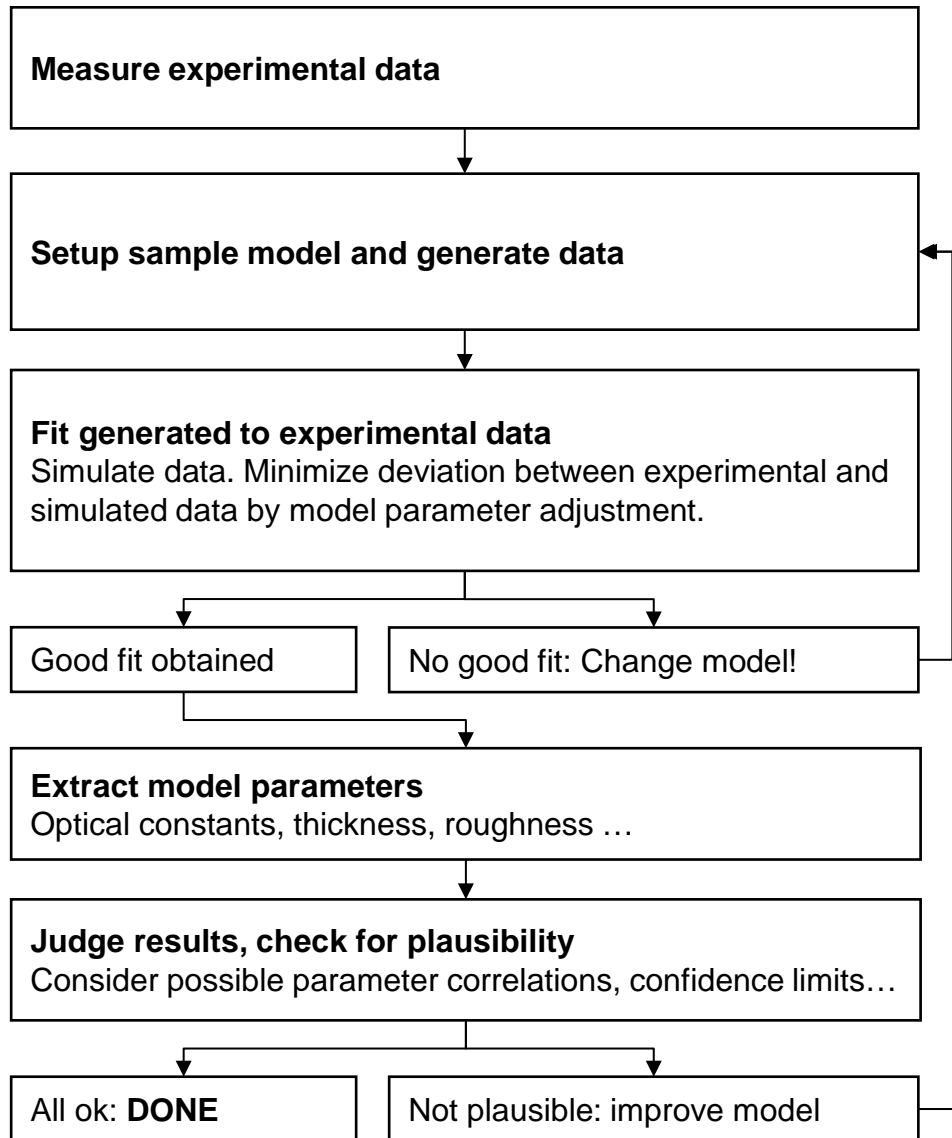
- **"Basic equation of ellipsometry"**  
(Here  $\rho$  is called "relative polarization ratio").

$$\rho = \tan \Psi \cdot e^{i\Delta} = \frac{R_p}{R_s}$$

# Elements of model analysis

- Flowchart of ellipsometry data analysis
- Parametric dispersion models:  
Description of optical constants vs. wavelength with few parameters

# Flow of ellipsometry data analysis



## User knowledge required:

- Basic sample structure: layers, interfacial layers, roughness
- Dispersion models  $n_i(\lambda)$ ,  $k_i(\lambda)$
- Initial parameter values

# The dispersion of permittivity and optical constants

The wavelength dependence or dispersion of optical constants is governed by

- Electronic mechanism
- Ionic mechanism
- Orientational mechanism

In the visible and UV spectral range resonances of electronic polarization occur.

Depending on material and spectral range different **dispersion models** are used. Advantage: description of the dispersion of optical constants with few model parameters.

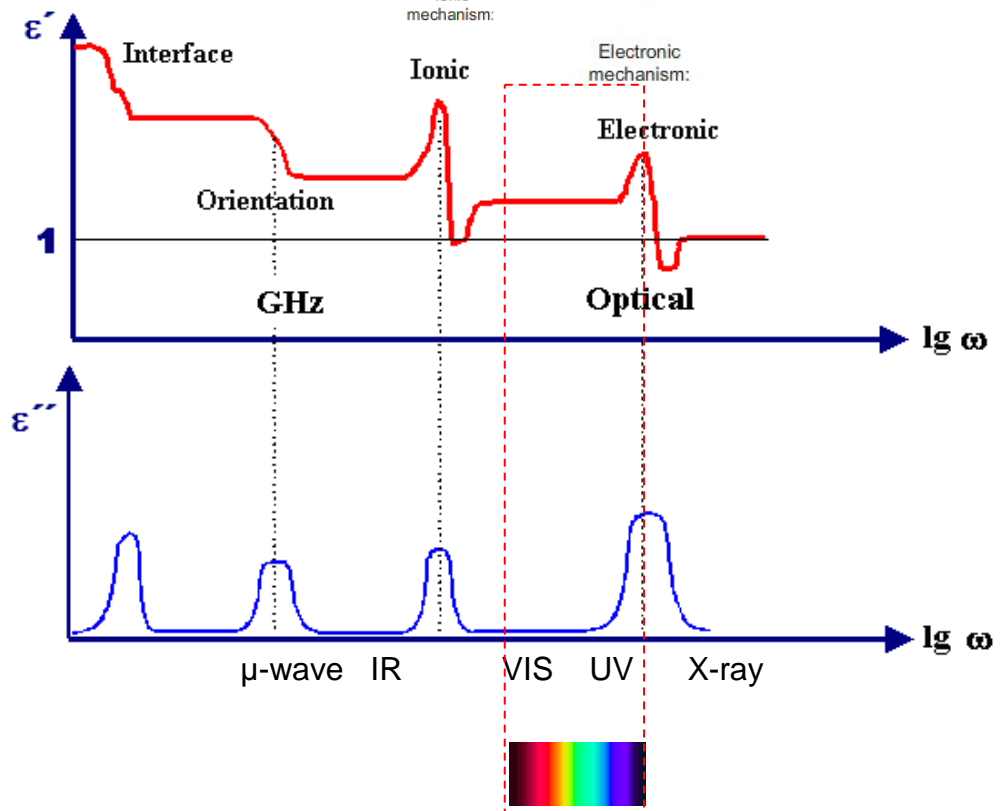
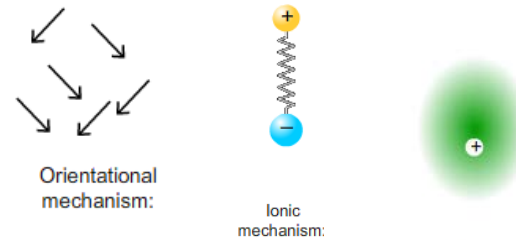


Image sources:

<https://www.doitpoms.ac.uk/tlplib/dielectrics/variation.php>

[http://www.tf.uni-kiel.de/matwis/amatermat\\_en/kap\\_3/backbone/r3\\_3\\_5.html](http://www.tf.uni-kiel.de/matwis/amatermat_en/kap_3/backbone/r3_3_5.html)

# Parametric models: Sellmeier model – normal dispersion

- Empirical model published in 1871 by Wolfgang von Sellmeier (1)
- „Sellmeier transparent“ dispersion for non-absorbing materials (2)

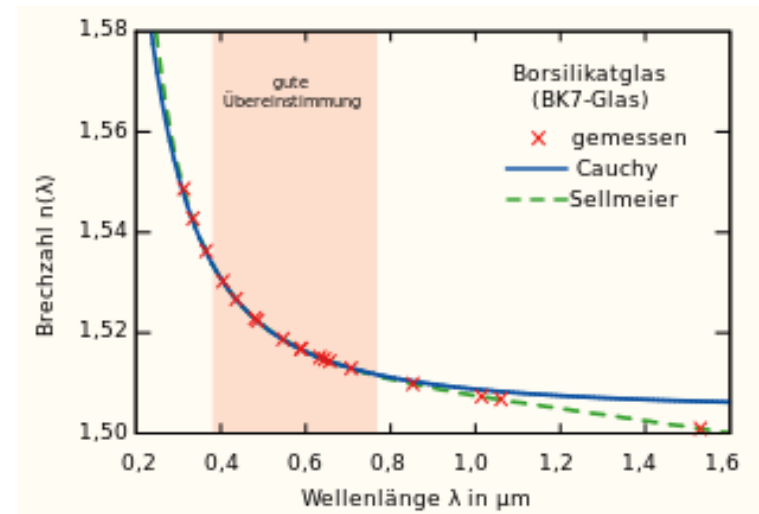
$$n^2(\lambda) = A + B \times \frac{\lambda^2}{\lambda^2 - \lambda_0^2}$$

$$k(\lambda) = 0$$

- „Sellmeier absorbing“ dispersion for weakly absorbing materials (2)

$$n^2(\lambda) = \frac{1 + A}{1 + \frac{10^4 \cdot B}{\lambda^2}}$$

$$k(\lambda) = \frac{C}{10^{-2} \cdot n \cdot D \cdot \lambda + \frac{10^2 \cdot E}{\lambda} + \frac{1}{\lambda^3}}$$



Comparison of Cauchy and Sellmeier fits to refractive index of BK7 glass (3)

## References:

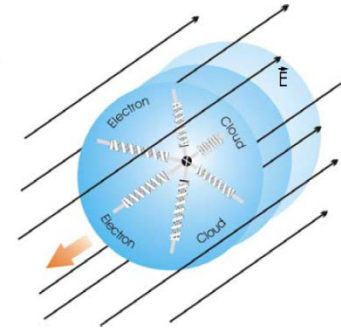
- (1) Wolfgang von Sellmeier: Zur Erklärung der abnormen Farbenfolge in Spectrum einiger Substanzen. In: *Annalen der Physik und Chemie*. 143, 1871, S. 272–282, [doi:10.1002/andp.18712190612](https://doi.org/10.1002/andp.18712190612)
- (2) [http://www.horiba.com/fileadmin/uploads/Scientific/Downloads/OpticalSchool\\_CN/TN/ellipsometer/Cauchy\\_and\\_related\\_empirical\\_dispersion\\_Formulae\\_for\\_Transparent\\_Materials.pdf](http://www.horiba.com/fileadmin/uploads/Scientific/Downloads/OpticalSchool_CN/TN/ellipsometer/Cauchy_and_related_empirical_dispersion_Formulae_for_Transparent_Materials.pdf)
- (3) <https://de.wikipedia.org/wiki/Sellmeier-Gleichung>

# Parametric models: Lorentz model - interband transitions

- Model named after Hendrik Antoon Lorentz (1853-1928), published 1878
- Model describes interaction of harmonic light field with bound electronic charges.
- Applicable to transparent and weakly absorbing materials (insulators and semiconductors).

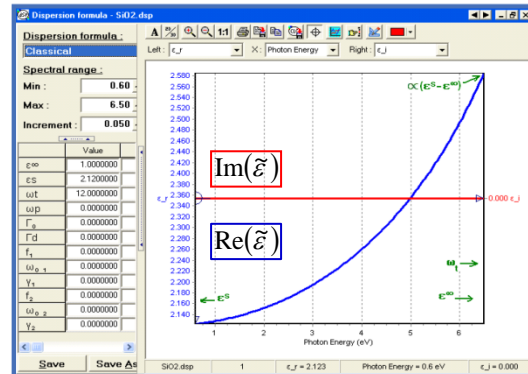
$$m \cdot \frac{d^2 \vec{r}}{dt^2} + m \cdot \Gamma_0 \cdot \frac{d\vec{r}}{dt} + m \cdot \omega_i^2 \cdot \vec{r} = -e \cdot \vec{E}_{loc}$$

$$\vec{r}(\omega) = \frac{1}{m} \cdot \frac{-e \cdot \vec{E}_{loc}}{(\omega_i^2 - \omega^2) + i \cdot \Gamma_0 \cdot \omega}$$

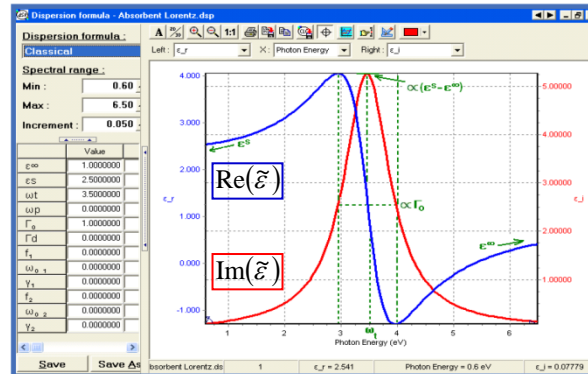


$$\tilde{\epsilon}(\omega) = \epsilon_\infty + \sum_{j=1}^N \frac{f_j \cdot \omega_{0j}^2}{\omega_{0j}^2 - \omega^2 + i \cdot \gamma_j \cdot \omega}$$

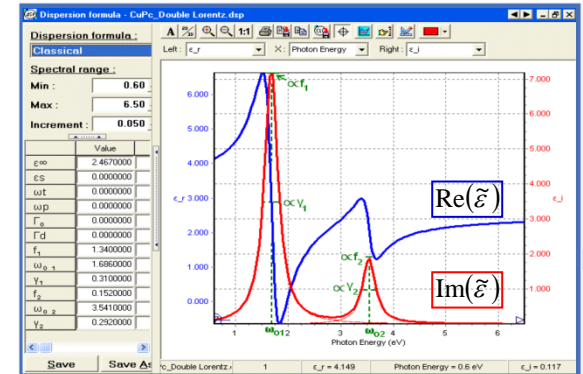
Representation of single-oscillator „Transparent Lorentz function“  
N=1,  $\gamma=0$ .



Representation of single-oscillator „Absorbing Lorentz function“



Representation of multiple-oscillator „Absorbing Lorentz function“



Source of images: (\*) [http://www.horiba.com/fileadmin/uploads/Scientific/Downloads/OpticalSchool\\_CN/TN/ellipsometer/Lorentz\\_Dispersion\\_Model.pdf](http://www.horiba.com/fileadmin/uploads/Scientific/Downloads/OpticalSchool_CN/TN/ellipsometer/Lorentz_Dispersion_Model.pdf)



# Parametric models: Drude model – free carrier absorption

- The model named after Karl Ludwig Paul Drude (1863-1906) was published 1900\*.
- It describes interaction of the light with free electrons. It can be regarded as limiting case of Lorentz model (restoring force and resonance frequency of electrons are null).
- Applicable to metals, conductive oxides and heavily doped semiconductors.
  - Does not take into account the notion of energy band gap  $E_g$  in semiconductors and quantum effects

## Parameters:

- Electron density, mass, charge
- Collision frequency
- Plasma frequency

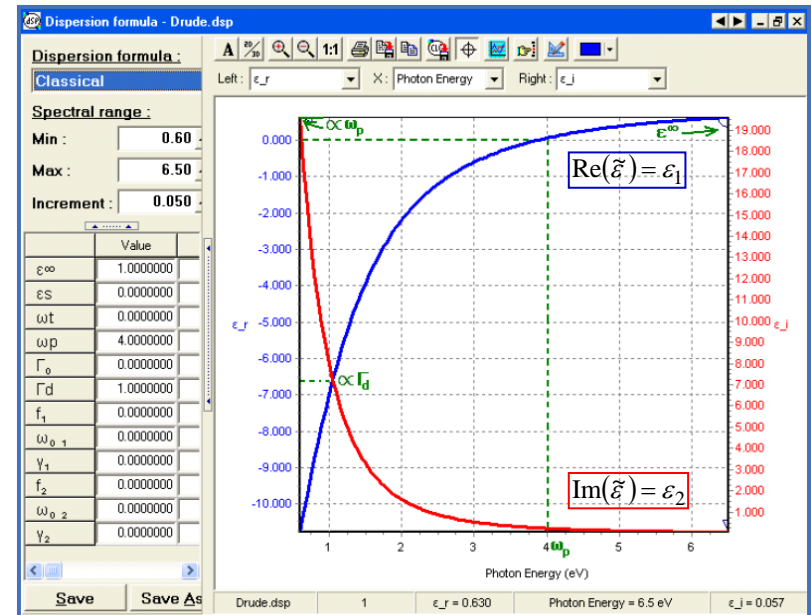
$$N, m$$

$$\Gamma \text{ [eV]}$$

$$\omega_p = \sqrt{\frac{N \cdot e^2}{m \cdot \epsilon_0}}$$

$$\tilde{\epsilon}(\omega) = 1 - \frac{N e^2}{m \epsilon_0} \cdot \frac{1}{(\omega^2 - i \Gamma_d \omega)} = 1 - \frac{\omega_p^2}{-\omega^2 + i \cdot \Gamma_d \cdot \omega}$$

$$\epsilon_1(\omega) = 1(\epsilon(\infty)) - \frac{\omega_p^2}{\omega^2 + \Gamma^2} \quad \epsilon_2(\omega) = \frac{\omega_p^2 \cdot \Gamma}{\omega \cdot (\omega^2 + \Gamma^2)}$$



## References

\* M. Dressel, M. Scheffler (2006). "Verifying the Drude response". *Ann. Phys.* 15 (7–8): 535–544. [Bibcode:2006AnP...518..535D](https://doi.org/10.1002/andp.200510198). [doi:10.1002/andp.200510198](https://doi.org/10.1002/andp.200510198).  
 Image: [http://www.horiba.com/fileadmin/uploads/Scientific/Downloads/OpticalSchool\\_CN/TN/ellipsometer/Drude\\_Dispersion\\_Model.pdf](http://www.horiba.com/fileadmin/uploads/Scientific/Downloads/OpticalSchool_CN/TN/ellipsometer/Drude_Dispersion_Model.pdf)

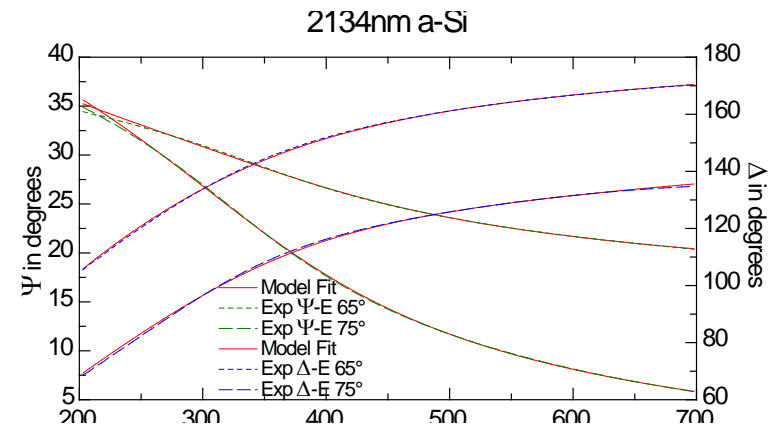
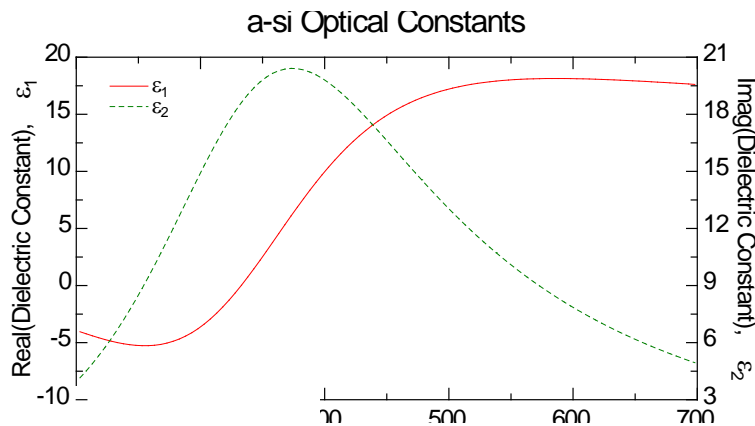
# „Tauc-Lorentz Model“: Amorphous materials in interband region

- Published by Jellison and Modine (1996): applicable to SiO<sub>2</sub>, Si<sub>3</sub>N<sub>4</sub>, a-Si, ...
- Kramers-Kronig consistent. Neglects intraband absorption.
- Yields meaningful parameters (e.g. opt. band gap E<sub>g</sub>).

$$\epsilon_{1TL}(E) = \epsilon_{1TL}(\infty) + \frac{1}{2} \frac{A}{\pi} \frac{C}{\zeta^4} \frac{a_{\ln}}{\alpha E_0} \ln \left[ \frac{(E_0^2 + E_g^2 + \alpha E_g)}{(E_0^2 + E_g^2 - \alpha E_g)} \right] - \frac{A}{\pi \cdot \zeta^4} \frac{a_{\text{atan}}}{E_0} \left[ \pi - \text{atan} \left( \frac{2E_g + \alpha}{C} \right) \right. \\ \left. + \text{atan} \left( \frac{-2E_g + \alpha}{C} \right) \right] + 2 \frac{AE_0 C}{\pi \zeta^4} \left\{ E_g (E^2 - \gamma^2) \left[ \pi + 2 \text{atan} \left( \frac{\gamma^2 - E_g^2}{\alpha C} \right) \right] \right\} \\ - 2 \frac{AE_0 C}{\pi \zeta^4} \frac{E^2 + E_g^2}{E} \ln \left( \frac{|E - E_g|}{E + E_g} \right) + 2 \frac{AE_0 C}{\pi \zeta^4} E_g \ln \left[ \frac{|E - E_g|(E + E_g)}{\sqrt{(E_0^2 - E_g^2)^2 + E_g^2 C^2}} \right],$$

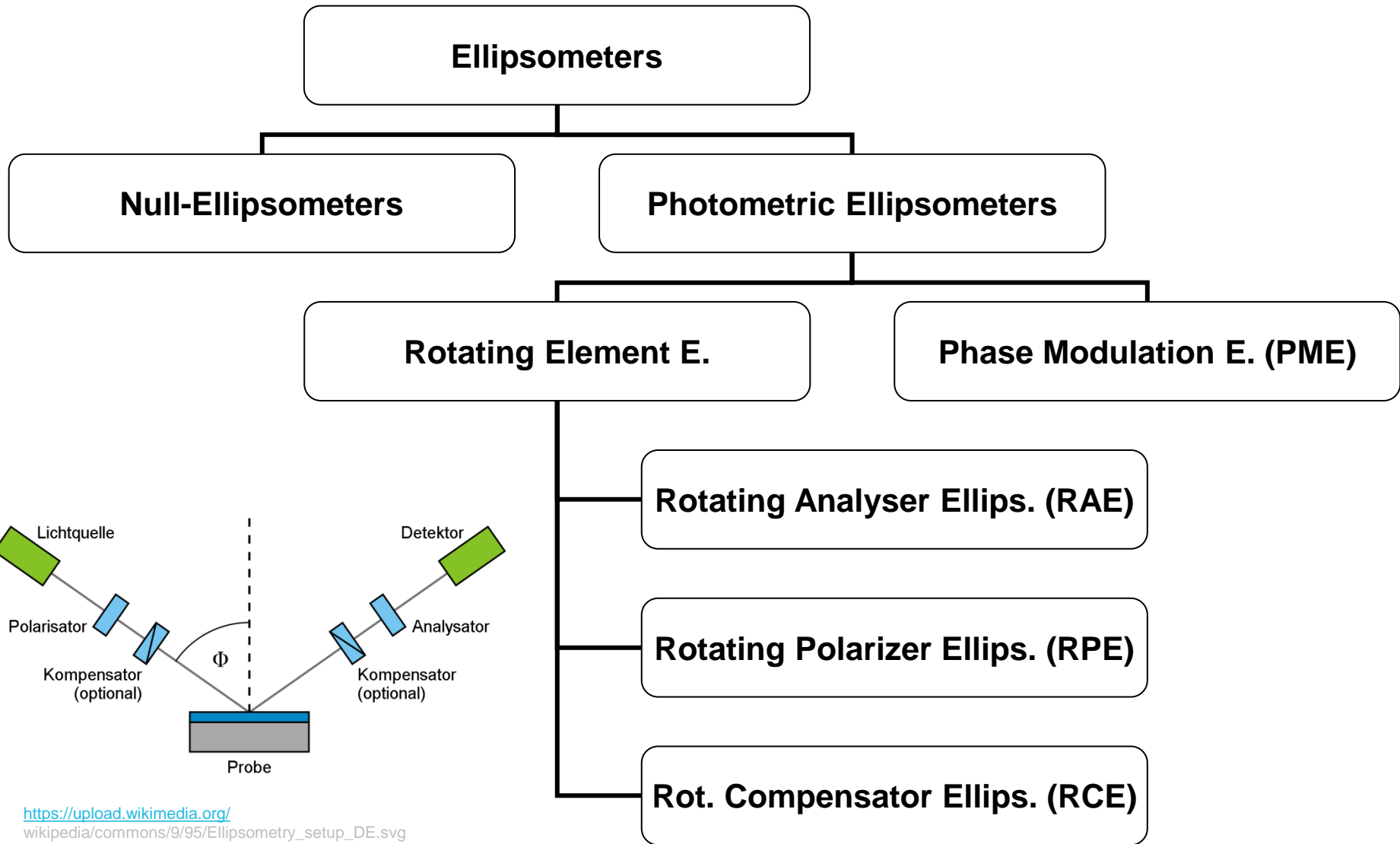
$$\epsilon_{2TL}(E) = \begin{cases} \frac{AE_0 C (E - E_g)^2}{(E^2 - E_0^2)^2 + C^2 E^2} \cdot \frac{1}{E}, & E > E_g, \\ 0 & E \leq E_g. \end{cases}$$

Jellison et al., Parameterization of the optical functions of amorphous materials in the interband Region, Appl. Phys. Lett. 69, 371 (1996); <http://dx.doi.org/10.1063/1.118064>



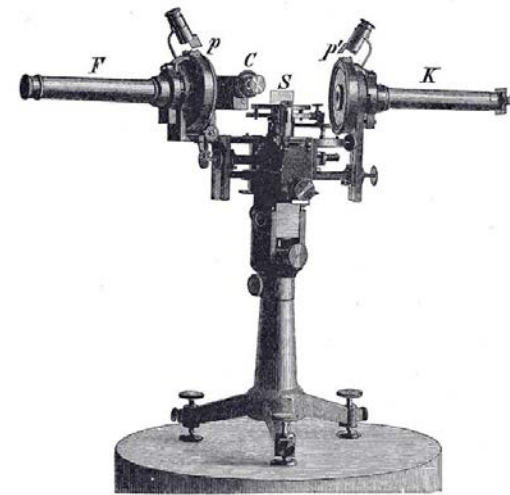
# Ellipsometry Instrumentation

# Classification of ellipsometers by operation principle



# Null Ellipsometer

- Change in polarisation caused by sample is compensated by adjusting polarizer and compensator so that the intensity at the detector detected is „nulled“.
- Now, sample parameters  $\psi$  and  $\Delta$  can be calculated from the known positions of polarizer, analyzer, and compensator.
- In principle no electronics is needed. Eye can be used as detector. Accurate, but slow technique.
- Until the 1970's the dominant concept. With advent of computers the faster photometric ellipsometers became more popular.
- Today the concept of Null ellipsometry is still used, e.g. in imaging ellipsometry for visualisation of very thin films.



Historical ellipsometer

Reference: Paul Drude, Lehrbuch der Optik, Leipzig, 1906

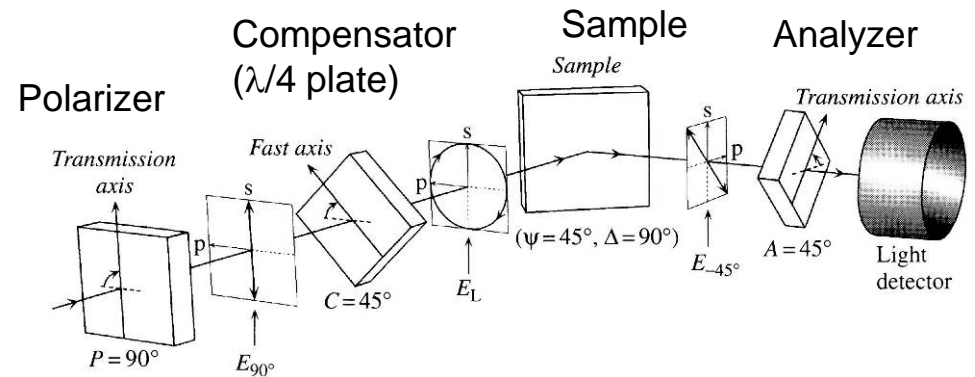


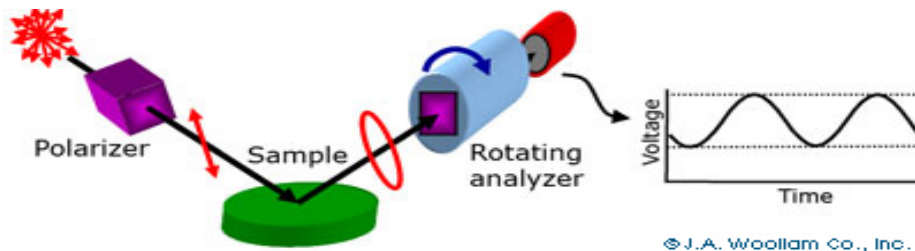
**Figure 4.15** Schematic diagram of measurement in null ellipsometry. In this figure, the  $(\psi, \Delta)$  values of a sample are assumed to be  $\psi = 45^\circ$  and  $\Delta = 90^\circ$ . In this measurement, the detected light intensity is zero.

# Photometric ellipsometers

Concept:

Either a rotating element (polarizer, analyzer, compensator) or an electro-optic phase modulator continuously modulate the beam. A computer calculates from the resulting harmonic intensity signal the ellipsometric data  $\Delta$  and  $\tan(\Psi)$ .

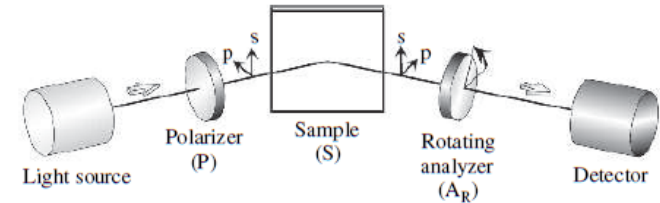
In contrast to the very fast phase modulating ellipsometers, rotating element ellipsometers may measure fast in a wide spectral range.



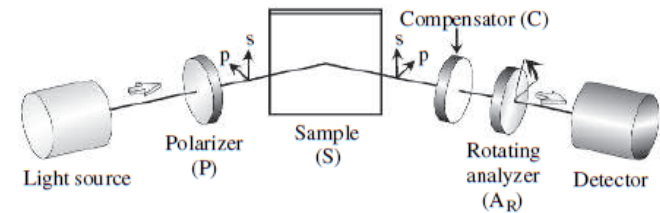
Source: Hiroyuki Fujiwara, Spectroscopic Ellipsometry - Principles and Applications, Wiley (2007)

## Different photometric ellipsometry variants

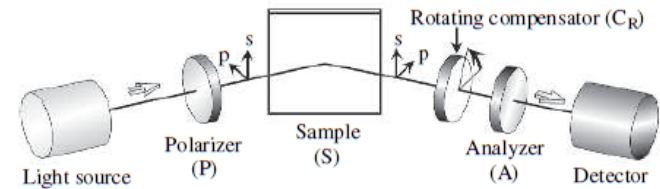
(a) Rotating-analyzer ellipsometry (PSA<sub>R</sub>)



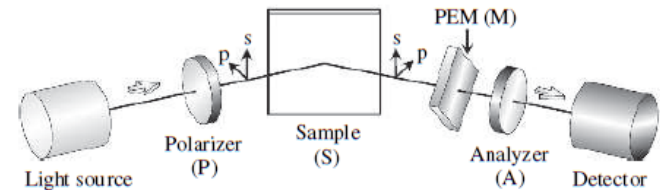
(b) Rotating-analyzer ellipsometry with compensator (PSCA<sub>R</sub>)



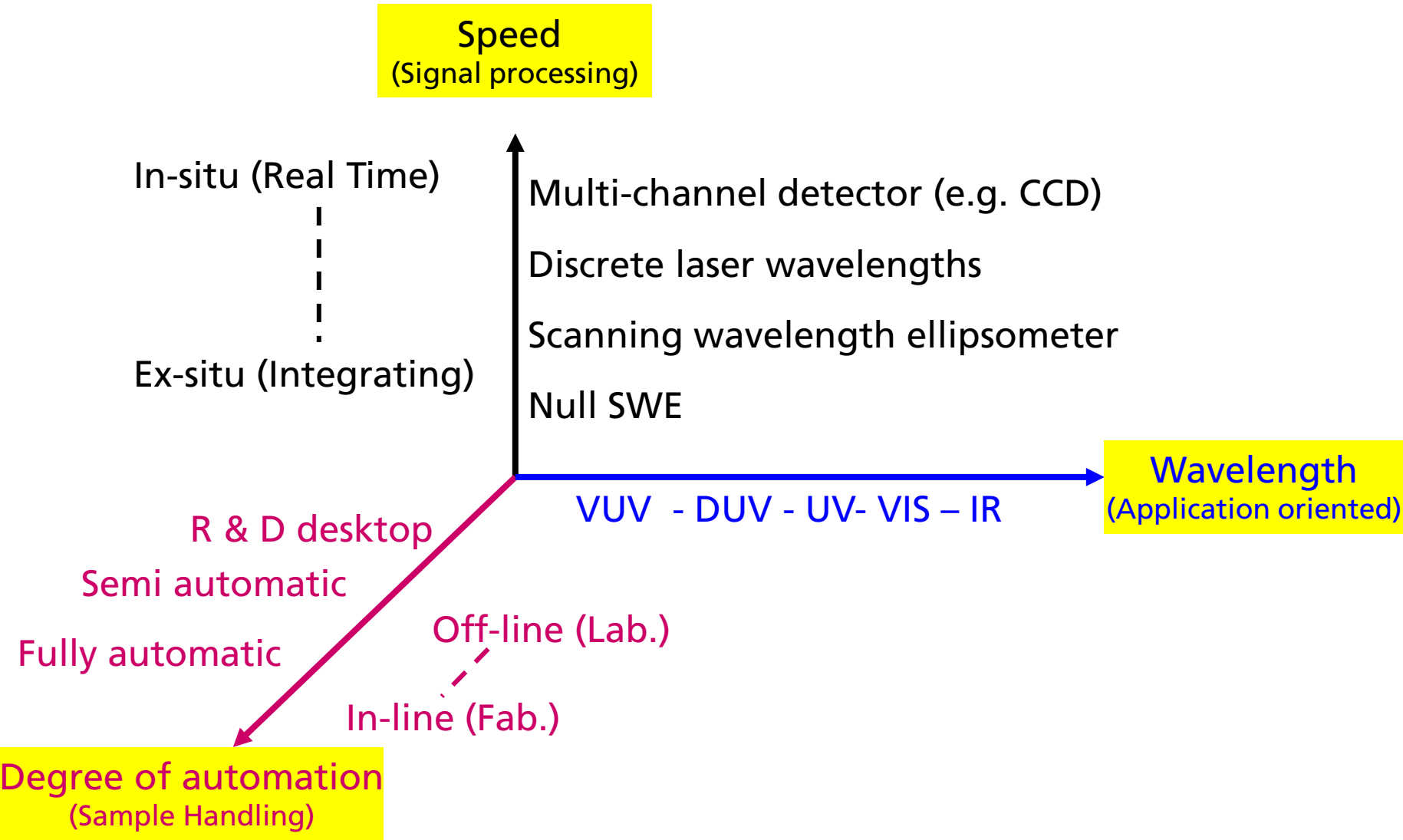
(c) Rotating-compensator ellipsometry (PSC<sub>R</sub>A)



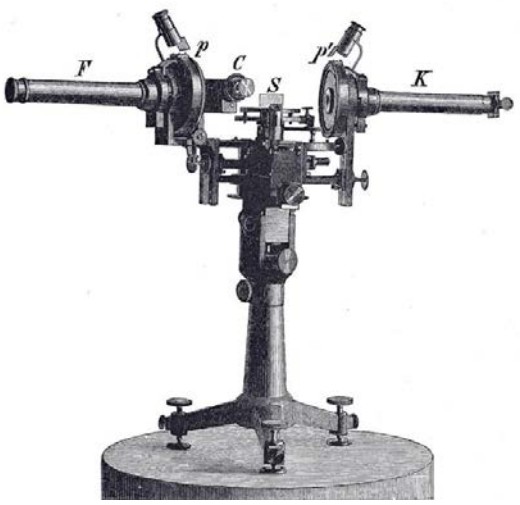
(d) Phase-modulation ellipsometry (PSMA)



# Ellipsometry systems: Classification by speed, wavelength range and automatization



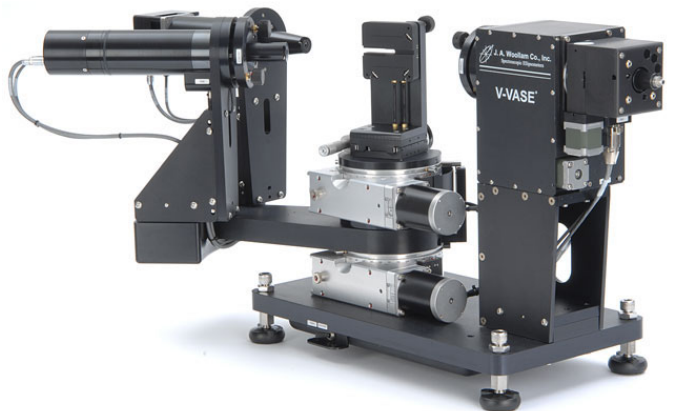
# Ellipsometry systems: Classification by Speed, Wavelength and Automatization



Historical ellipsometer  
Reference: Paul Drude, Lehrbuch der Optik, Leipzig, 1906



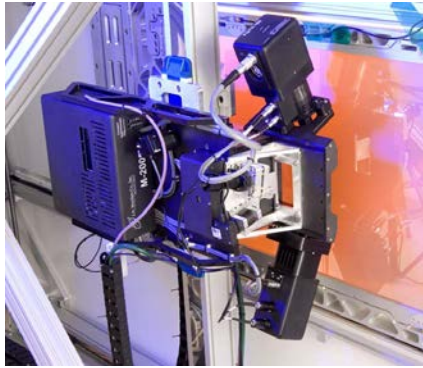
Alpha-SE (Woollam):  
Multi-wavelength 380-900nm, angles: 65°, 70°, 75° or 90°  
<https://www.jawoollam.com/products>



VASE (Woollam):  
Scanning wavelength 190-1700nm, variable angle SE  
<https://www.jawoollam.com/products>



IR-VASE MARK II (Woollam) :  
Variable angle, scanning wavelength SE. Range 1.7-33µm  
<https://www.jawoollam.com/download/pdfs/ir-vase-brochure.pdf>



M2000 (Woollam) : real-time SE with high speed  
CCD detector  
<https://www.jawoollam.com/products/m-2000-ellipsometer>



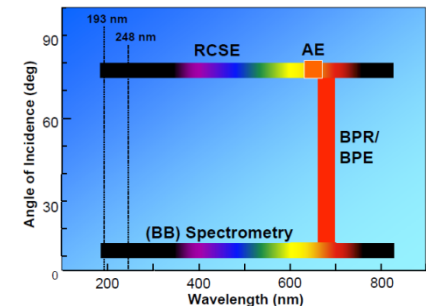
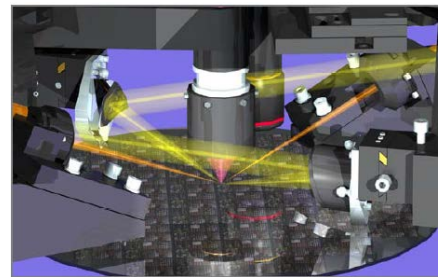
UVISEL 2 VUV (Horiba): 147-2100nm VUV-NIR SE  
<http://www.horiba.com/scientific/products/ellipsometers/spectroscopic-ellipsometers/uvisel-vuv/uvisel-2-vuv-23265/>



# In-line ellipsometer system for wafer fabs: Thermawave Opti-Probe 5240

(Status of 2005)

- Beam Profile **Reflectometer** (BPR)
  - Solid-state laser
  - Angular-dependent film reflectivity data
- Beam Profile **Ellipsometer** (BPE)
  - BPR source and optics
  - Basic polarization data w/ smallest box size
- Absolute **Ellipsometer** (AE)
  - He/Ne laser
  - High precision ellipsometer for the very thinnest films
- Broad-Band **Spectrometer** (BB)
  - Continuous spectral source (190-840nm)
  - Provides spectroscopic characterization of materials
- DUV Rotating Compensator **Spectroscopic Ellipsometry** (RCSE)
  - Continuous spectral source (190-840nm, same source as BB)
  - Complex spectral and phase data for initial multiple parameter characterization of film stacks



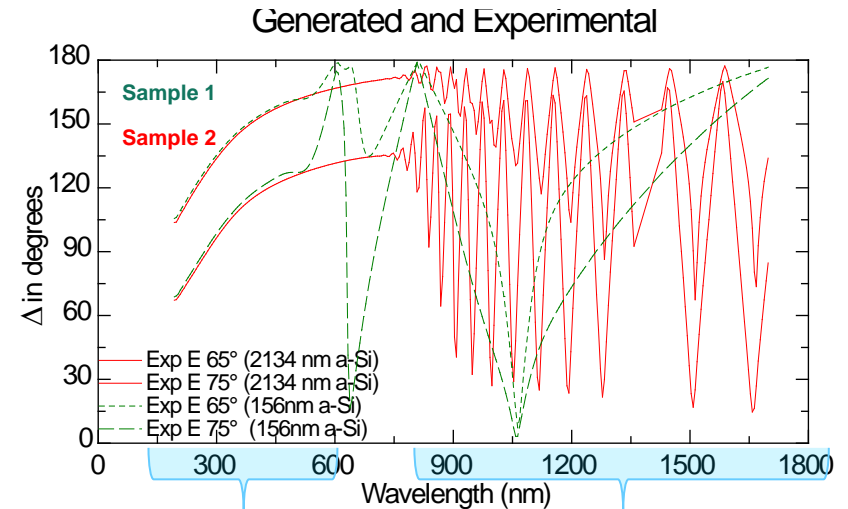
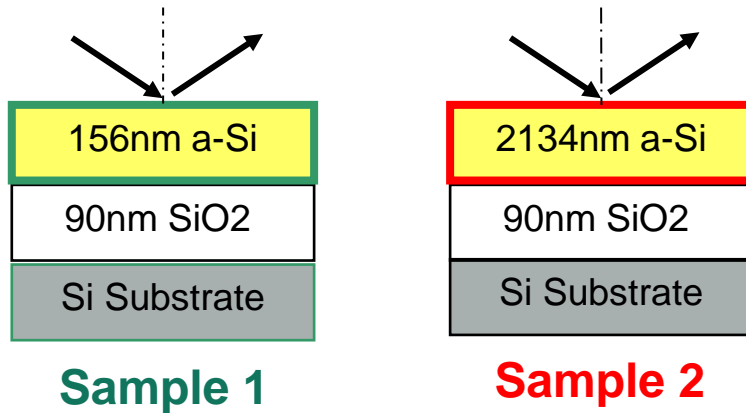
# Potential of Spectroscopic Ellipsometry

# EXAMPLARY APPLICATIONS OF ELLIPSOMETRY

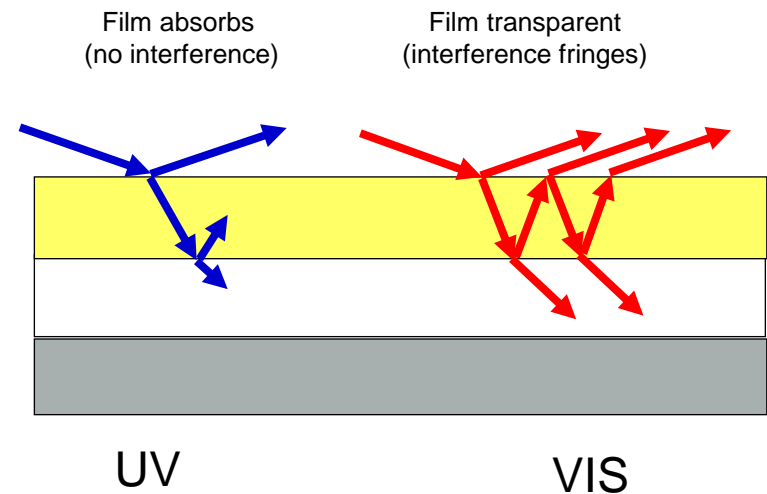
# Example: Spectroscopic Ellipsometry of a-Si - Thickness measurement in transparent spectral region

# Example: Ellipsometry of UV absorbing films

## Thickness measurement of a-Si films



- In DUV-UV where a-Si is strongly absorbing, both datasets coincide:
- Spectra are independent of a-Si thickness, since no reflected light from lower film interface is measured.
- In the transparent region, thickness-dependent interferences are observed.
- Narrow / wide spacing of fringes indicates thinner / thicker film.

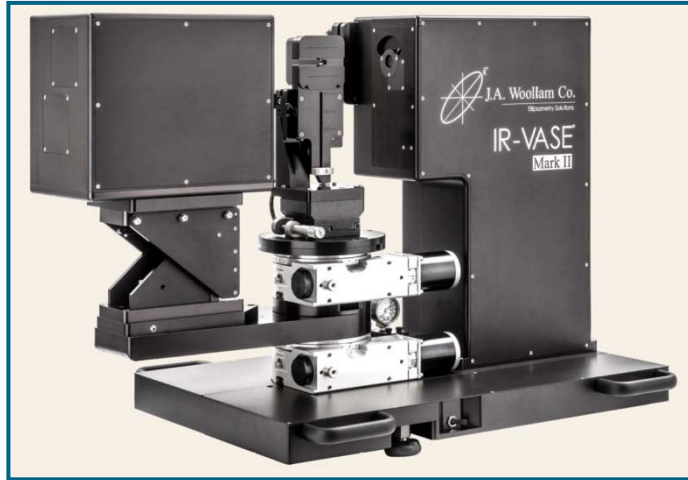


**Example:**

**Infrared spectroscopic ellipsometry:  
Chemical analysis of nm-thick films**

# Spectroscopic ellipsometry for specific sample properties

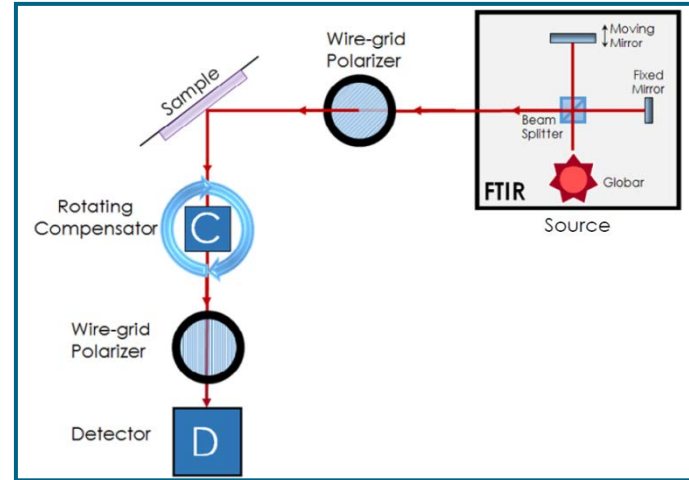
## Thickness and chemical nature of nm-thick films by VASE in IR spectral range



### Woollam IR-VASE „Mark II“

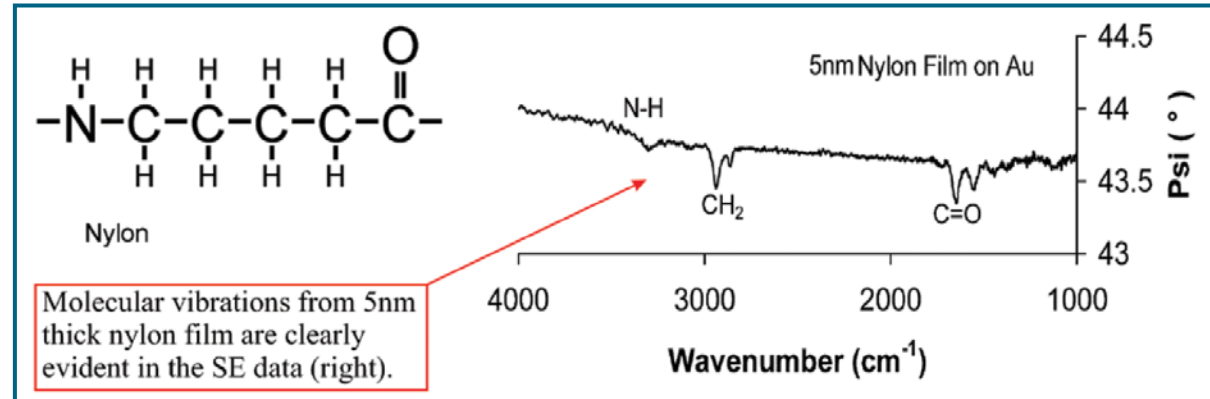
Spectral Range:  
1.7-30 $\mu\text{m}$  /  
333-5900 $\text{cm}^{-1}$

Angular range:  
32..90°



### Benefits of IR-VASE

- n,k in measured spectral range w/o need to extrapolate beyond measured range (as for Kramers-Kronig analysis)
- High sensitivity to thickness and chemical composition
- No reference sample / baseline measurement required.



# Summary on Ellipsometry

- Probed is the change in polarization induced by reflection (transmission) of light by a smooth sample.
- By means of model-analysis sample parameters can be deduced.
  - Precise thickness (down to few nm), and roughness of thin films and multilayers
  - Spectroscopic ellipsometry: dielectric constants from VUV to IR
- Advantages of the method are
  - Non-destructive
  - Real-time measurements possible



# X-ray reflectometry

- Measurement principle
- Examples

# X-ray reflectometry: What is it all about

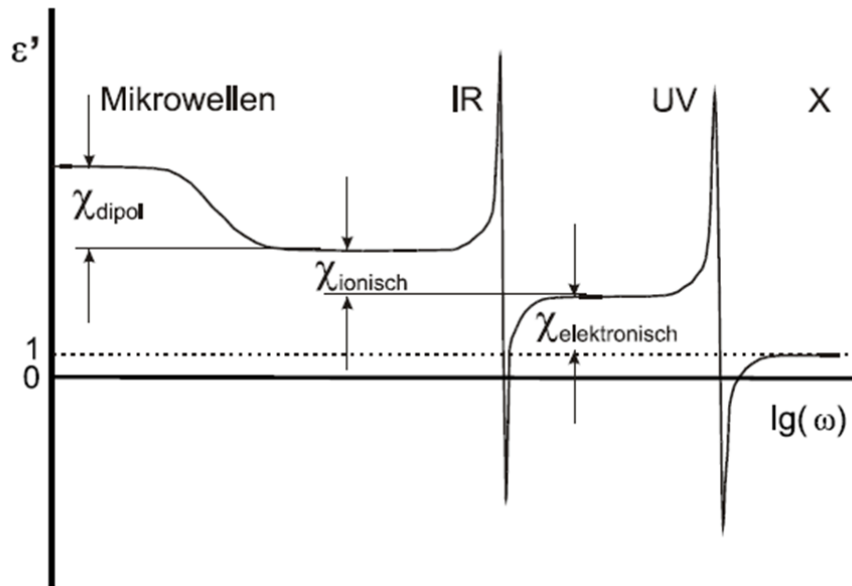
- X-ray reflectometry is a measurement of reflectance vs. angle near grazing incidence at a fixed wavelength in the hard x-ray range.
- The technique allows to investigate
  - thickness of single or multilayers incl. metals
  - interface and surface roughness
- Limitations
  - Requires samples of low roughness
  - Max. measurable thickness limited by angular resolution of primary beam and goniometer. (Typically <150nm.)
  - Size of measurement spot is > some mm<sup>2</sup>

# X-ray reflectometry: What is it all about

- For x-rays all materials are quasi transparent. Their optical indices can be expressed as

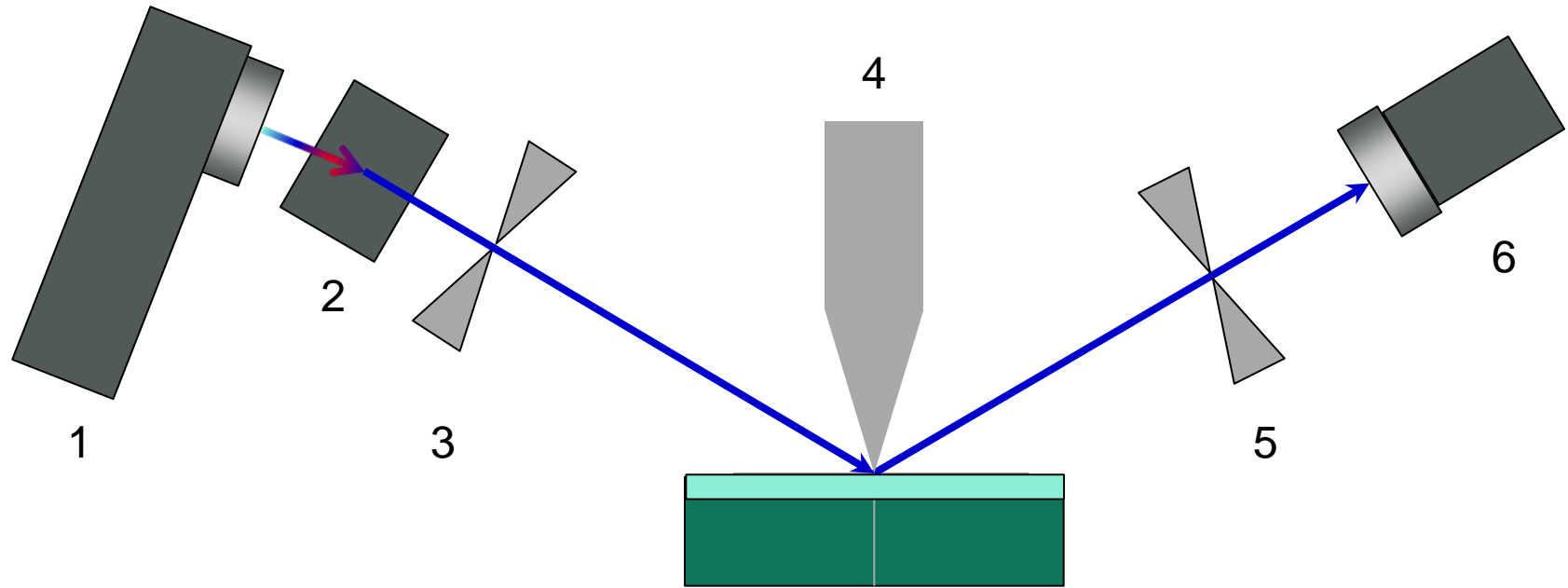
$$N=1-\delta+i\beta, \text{ where } \delta, \beta \text{ are small } (\sim 10e-5 \text{ ..}10e-6)$$

- Since air is optically more dense than any film, total external reflection is observed at small angle of incidence.



W. Kriegseis, Röntgen-Reflektometrie zur Dünnschichtanalyse, 2002  
<http://www.uni-giessen.de/cms/fbz/fb07/fachgebiete/physik/lehre/fprak/anleitungen/reflekt2>

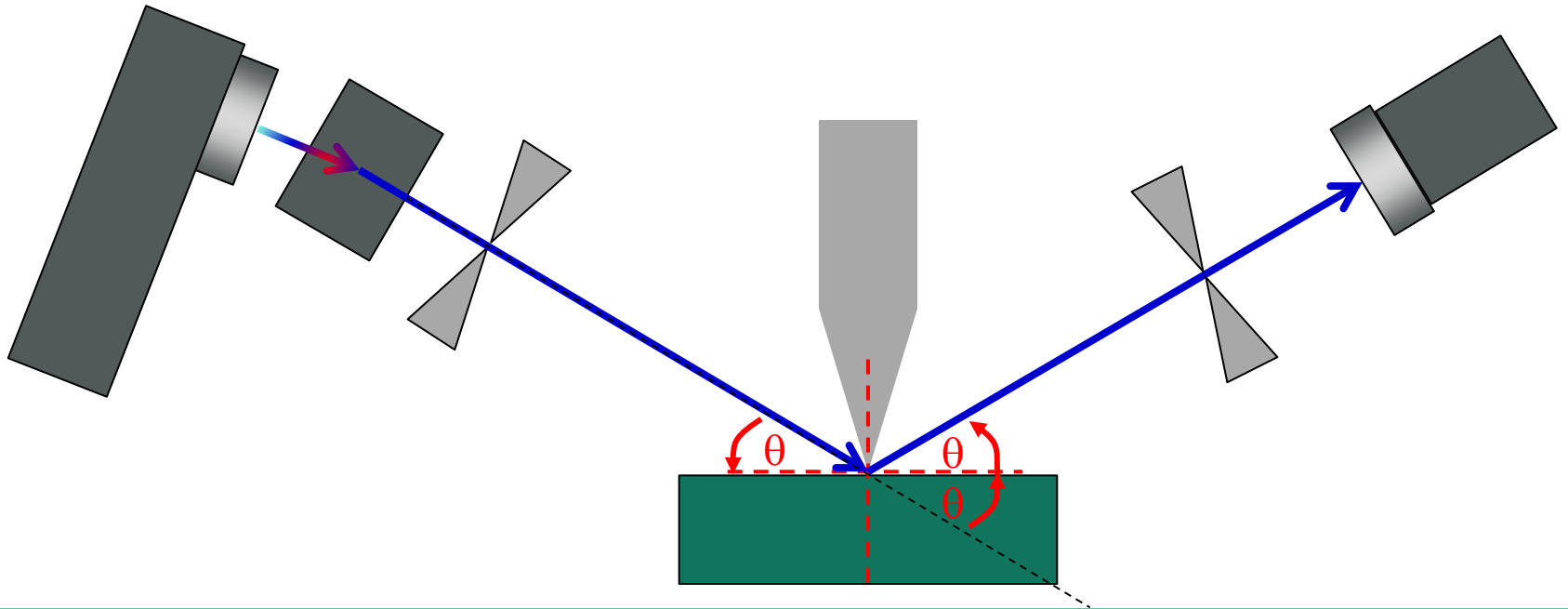
# X-ray reflectometry: Measurement setup



#	Component	Function
1	X-ray tube	Emitts divergent polychromatic radiation (char.+braking radiation)
2	Göbel mirror	Multilayer mirror on parab. substrate, spectral filter, collimates beam
3	Slit 1	Beam limiter
4	Knife edge absorber	Limits the analyzed area on sample. Almost touches surface.
5	Slit 2	Beam limiter
6	Detector	Intensity measurement. ~5-6 decades dynamic range.

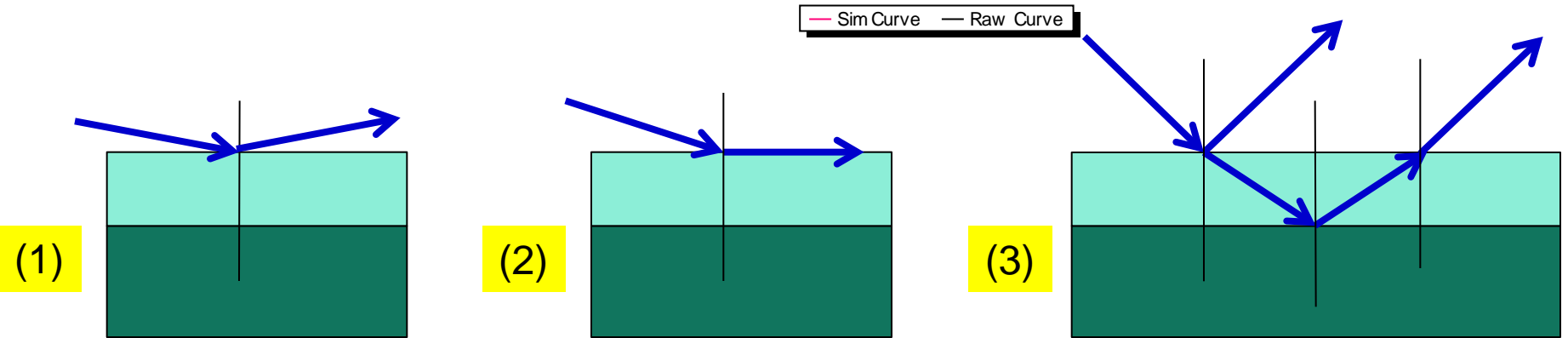
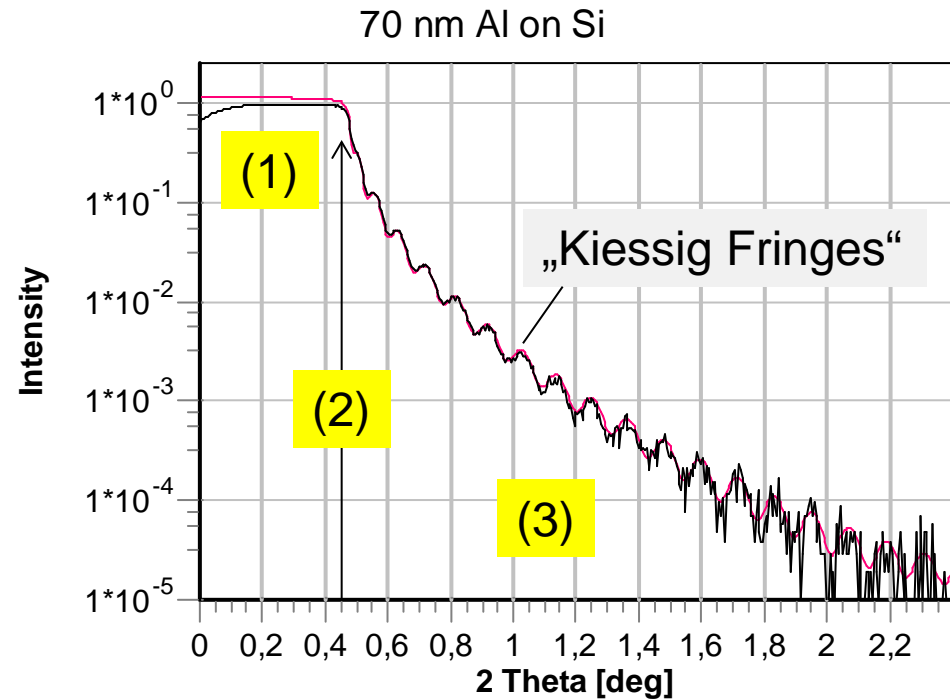
# X-ray reflectometry: Measurement principle

- In a setup with fixed x-ray tube, sample and detector are rotated about a common axis of rotation by angle  $\theta$  and  $2\theta$  respectively.
- Typical values:  $\theta$  range 0..3 deg, step width  $d\theta \sim 0.001$  to 0.05 deg, depending on film thickness to be measured.



# X-ray reflectometry: Understanding data features

1. At small angle of incidence  $\Theta$ , total external reflection occurs.
2. At a „critical angle“  $\Theta_c$ , evanescent waves exist at the sample surface, but still no beams propagate into the film.  $\Theta_{crit}$  correlates with mass density of (the top layer of) the sample. Examples:  $\Theta_{c,Be}=0,186^\circ$ ,  $\Theta_{c,Pt}=0,583^\circ$
3. At higher  $\Theta$ , diffracted x-rays enter the film, are reflected at interfaces, and leave the sample parallel to the beam reflected at the top surface. Interference causes oscillations in intensity as  $\Theta$  is varied. From the period of oscillations the film thickness is derived.



# X-ray reflectometry: Sensitivity to sample parameters

## Single Metal Film + Substrate Pt film on Si (Simulations)

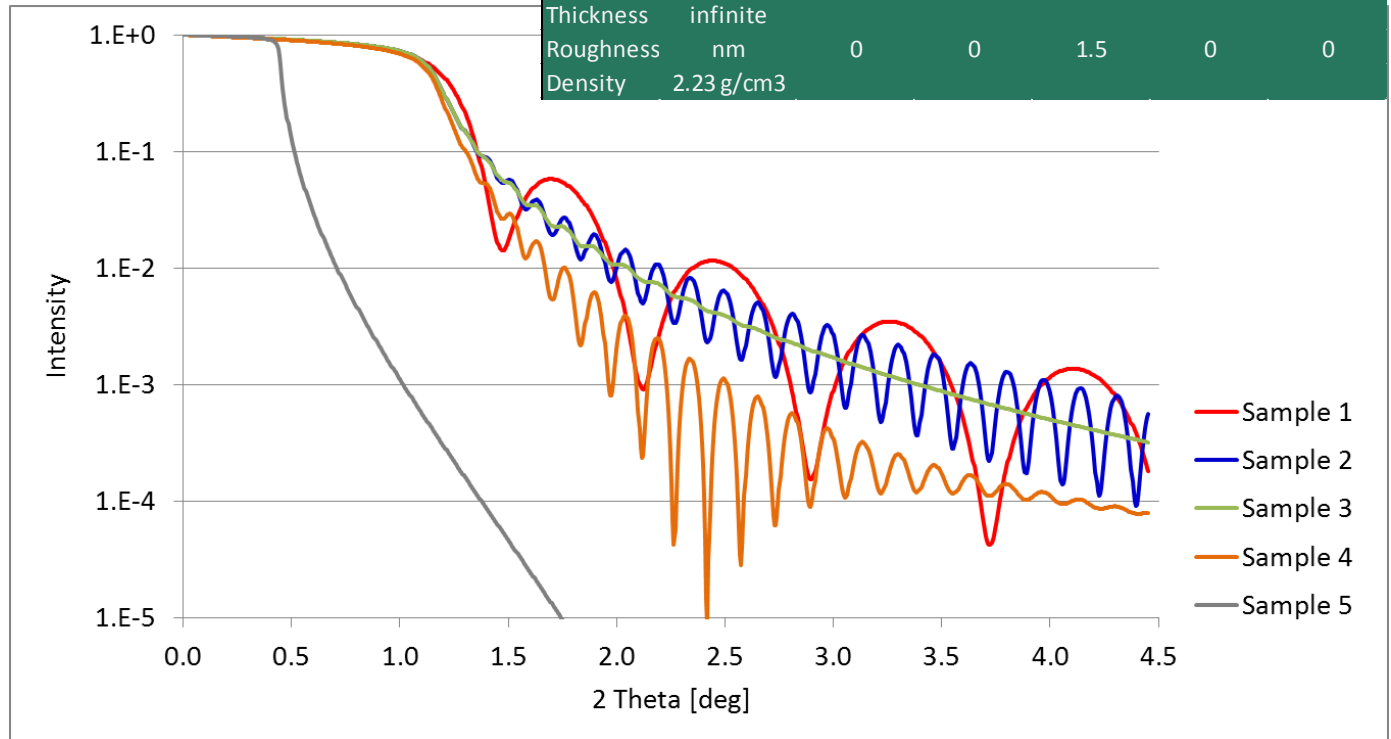
### XRR Method is sensitive to

- Film Thickness
- Film Roughness
- Film density
- Interface Roughness

Legend:

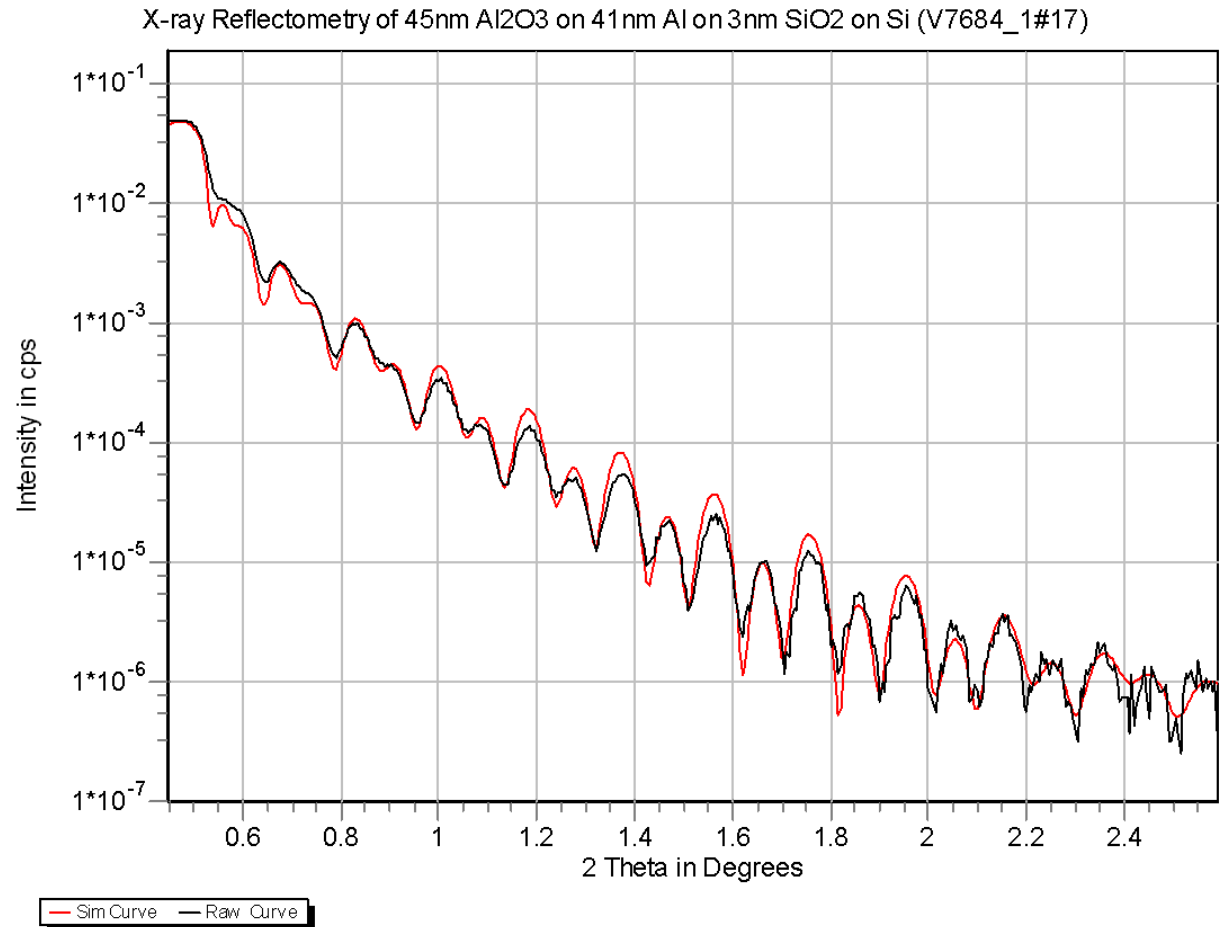


Platinum		Sample1	Sample2	Sample3	Sample4	Sample5
Thickness	nm	10	50	50	50	no Pt film
Roughness	nm	0	0	0	1.5	film
Density	g/cm <sup>3</sup>	21.44				
Silicon		Sample1	Sample2	Sample3	Sample4	Sample5
Thickness	infinite					
Roughness	nm	0	0	1.5	0	0
Density	g/cm <sup>3</sup>	2.23				



# X-ray reflectometry: Application – Reflectors for MEMS

## Bilayer + Substrate Al<sub>2</sub>O<sub>3</sub>+Al on Si





# Summary on X-ray reflectometry

- Probed is x-ray reflectance as function of angle or energy.
- Samples are smooth, unstructured.
- By means of model-analysis sample parameters can be deduced.
  - Very precise thickness (down to sub-nm films), and roughness of thin films and multilayers.
  - Due to low absorption of x-rays, even metal films can be measured.
  - Film density can be estimated.

# Outline

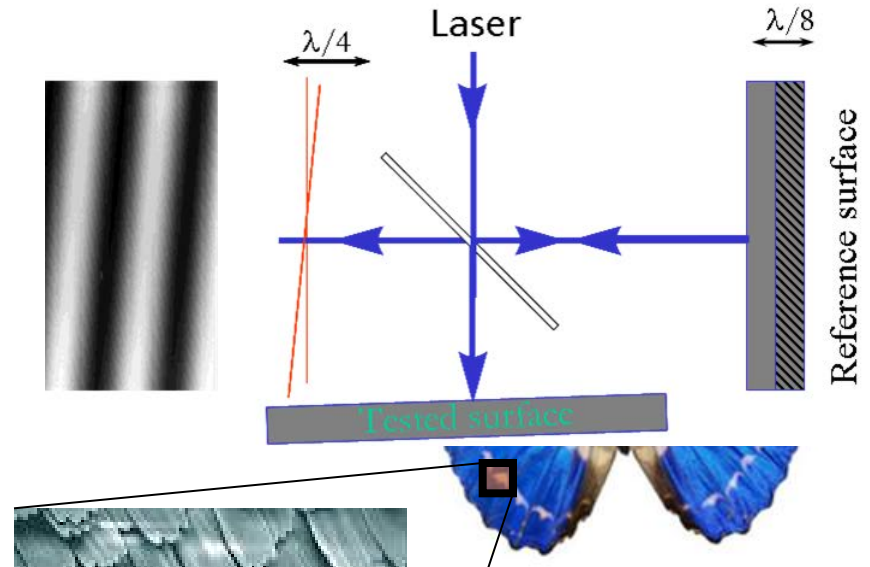
- Ellipsometry
- X-Ray reflectometry
- White light interferometry
  - Application to diffractive MEMS

# WHITE LIGHT INTERFEROMETRY (WLI)

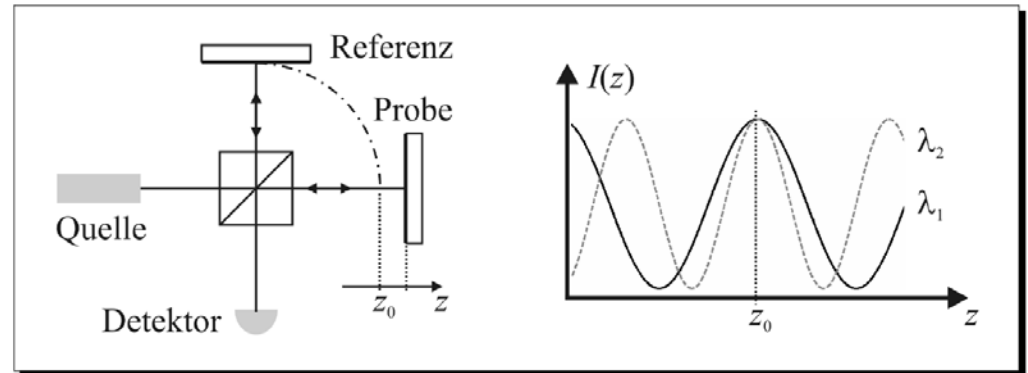
- Principle & Instrumentation
- Application to diffractive MEMS

# Introduction

- Interference of light can be used for the precise measurement of surface profiles “phase shift interferometry”
  - Key: monochromatic light



- Does it make sense to use broad spectra to extract signals of nanostructures unlike classical phase-shift interferometry ?

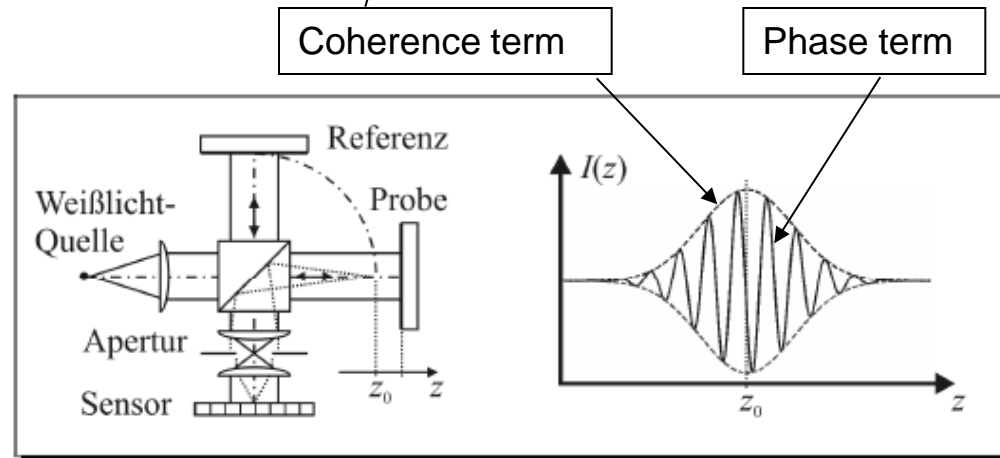


# Principle

- Superposition of two polychromatic waves
  - Interference signal
    - Standard phase term
    - Spectral coherence function as envelope (key parameter – coherence length  $l_c$ )
  - Gain
    - Direct determination of the object position - "envelope maximum"
- (Resolve ambiguity of phase shift interferometry)

$$E_{Sensor} = E_{reference} + E_{object}$$

$$I_{sig}(z) = I_1 + I_2 \cdot \gamma_{12}(z - z_0) \cos[k_0(z - z_0) + \alpha_{12}]$$

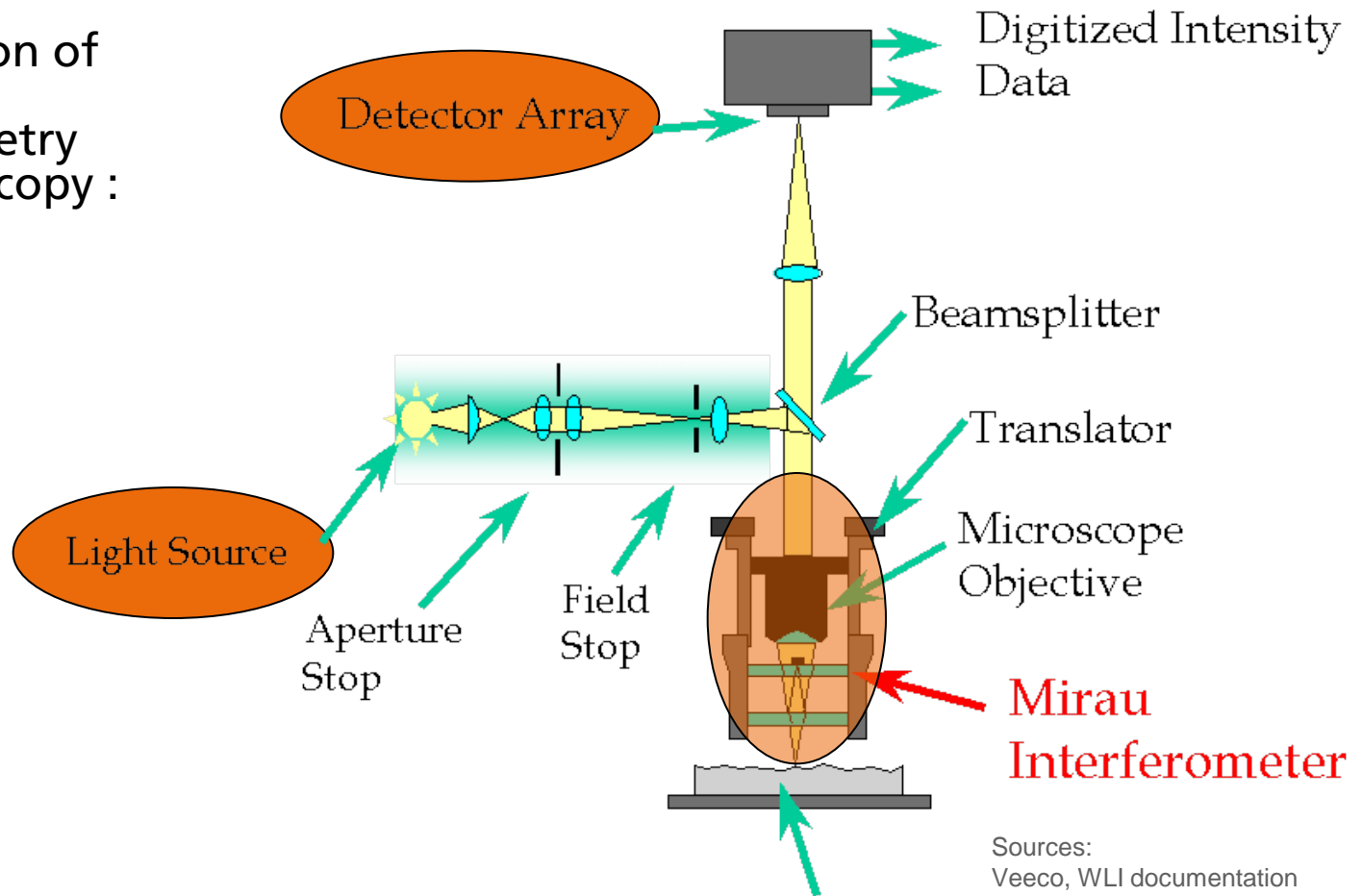


Sources:  
M. Hering, Dissertation (2007) Heidelberg

# INSTRUMENTATION

# Optical analysis of *micro- and nanostructures*

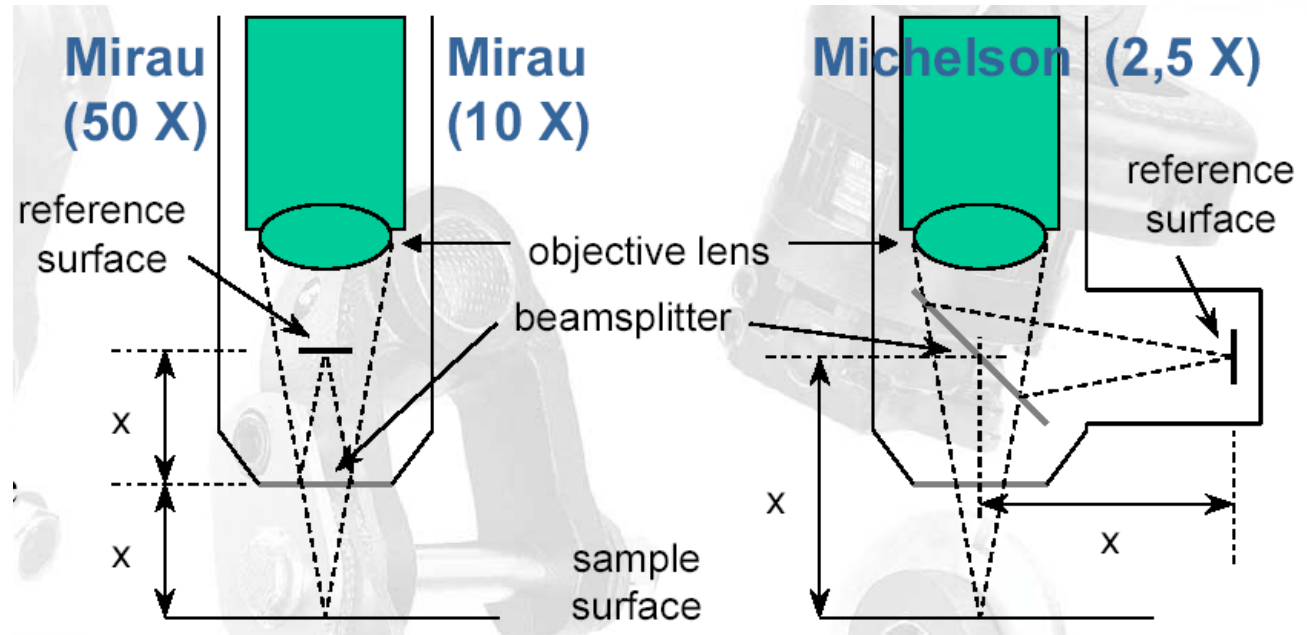
- Combination of white light interferometry and microscopy :



Sources:  
Veeco, WLI documentation

# Optical analysis of *micro- and nanostructures*

- Optical magnification determines interferometry-principle
- Resolution
  - < 1nm vertical Interferometry
  - <1  $\mu\text{m}$  lateral "Microscopy"
- Through-glass measurement possible



Sources:  
Veeco, WLI documentation

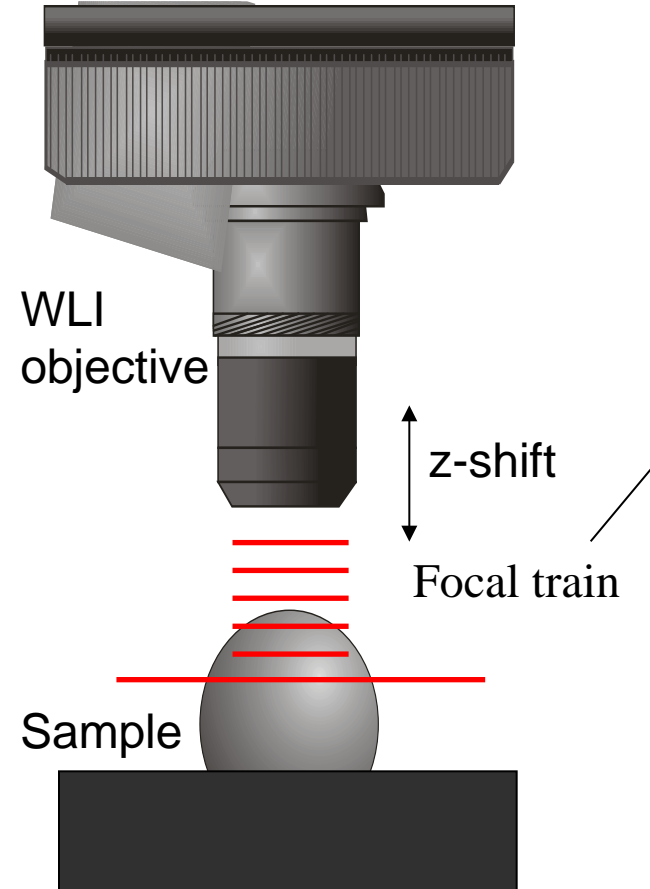


# Optical analysis of *micro- and nanostructures*

Illustrated measurement scan:

- Movement of sample, objective or reference plane
- Record intensity at each camera-pixel
- Analyze the pixel-intensity while moving through focus "interferogram"

→ How to extract the surface topography *at each pixel*?



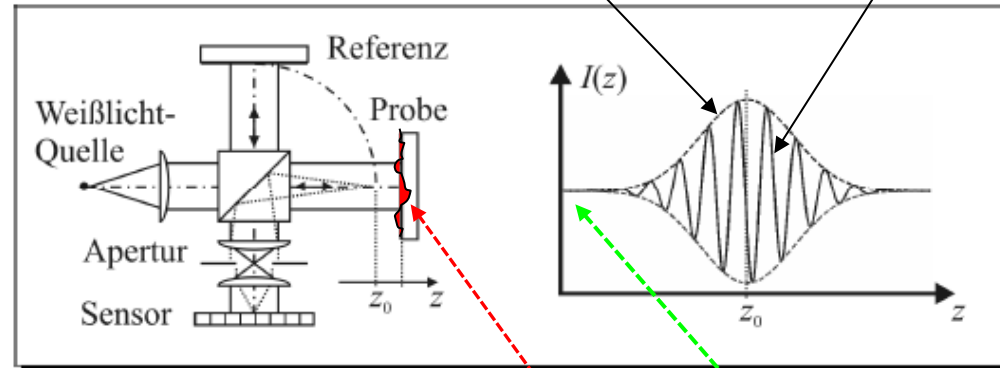
Sources:  
Veeco, WLI documentation

# The WLI signal

$$I_{sig}(z) = I_1 + I_2 \cdot \gamma_{12}(z - z_0) \cos[k_0(z - z_0) + \alpha_{12}]$$

Coherence term

Phase term



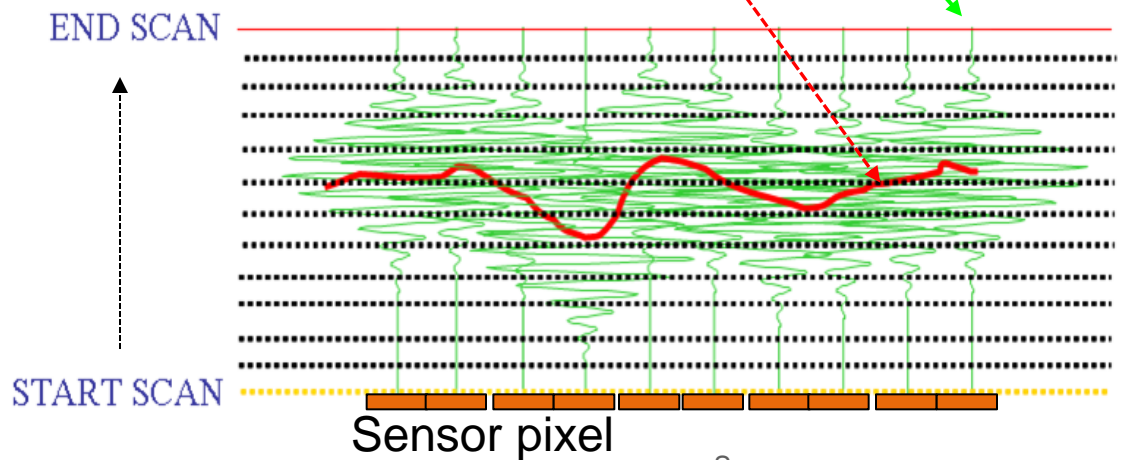
■ Best focus corresponds to zero optical path difference

■ → straight forward height determination by z-scan

■ SW extraction of envelope maxima

- Hilbert transform
- Wavelet transform
- other techniques

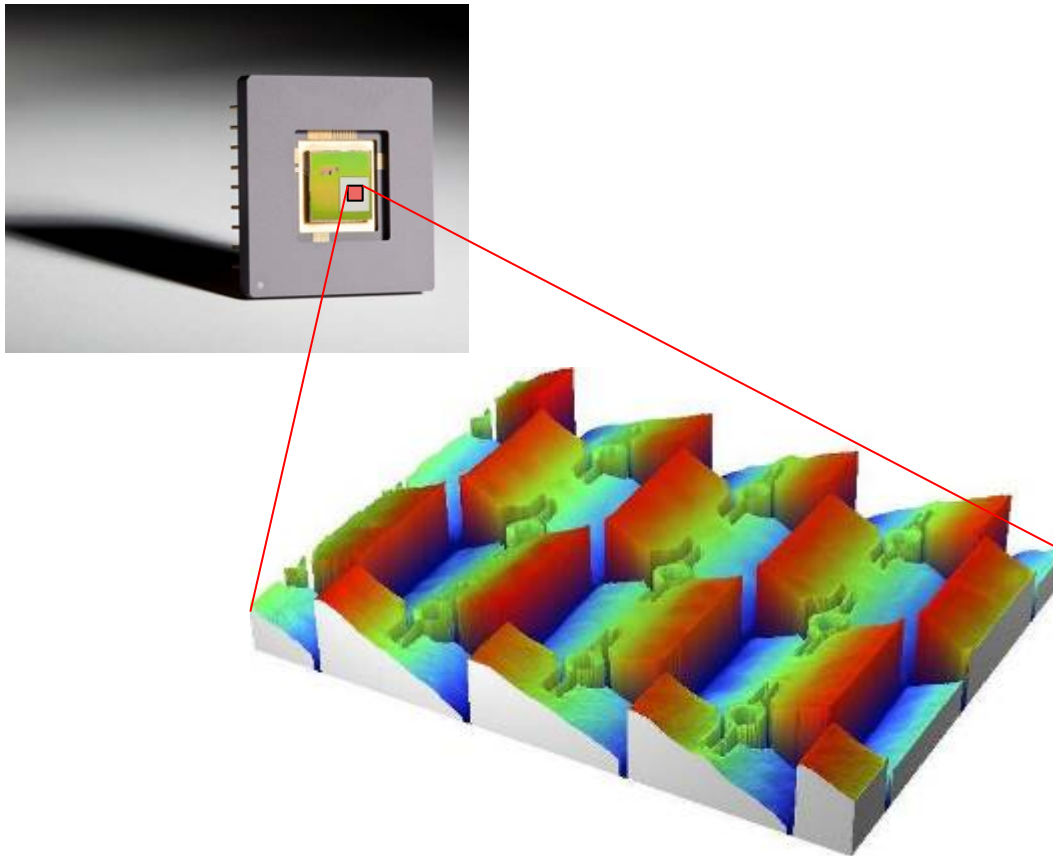
*What is the "surface"?*



Sources:  
Zygo, WLI documentation

# Optical analysis of *micro- and nanostructures*

- Measurement section of a MEMS array – torsion micromirrors  
(Field of view  $70\ \mu\text{m} \times 50\ \mu\text{m}$ ,  $0.2\ \text{nm}$  vertical resolution)



## Summary - White Light Interferometry (WLI)

- WLI is an optical method measuring the phase-change of light
- Topography properties can be directly determined - without user interaction.
- Advantages
  - $< 1\text{nm}$  (z-resolution) with dynamic range  $>100\mu\text{m}$
  - Non-destructive
  - Direct and parallel data acquisition without model assumption
  - Inspection of optical constants & thickness of structured thin films optionally
- Typical application ?

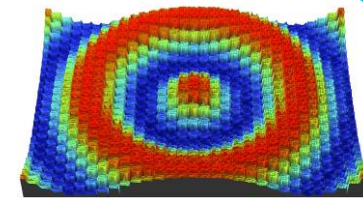
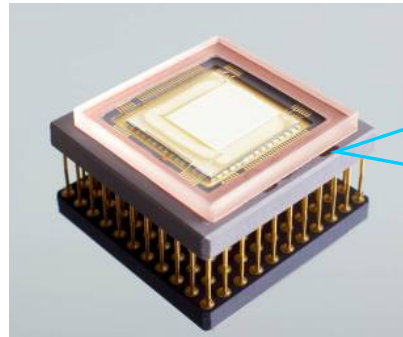
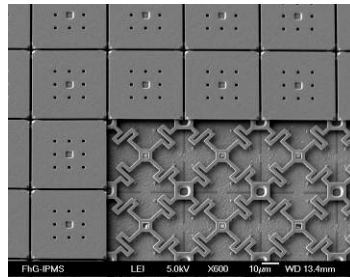
# APPLICATION EXAMPLE:

## WLI characterization and MEMS micromachining

# Overview: Micromirror Arrays – diffractive MEMS modulators

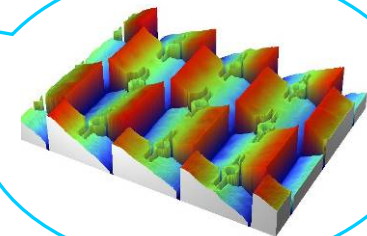
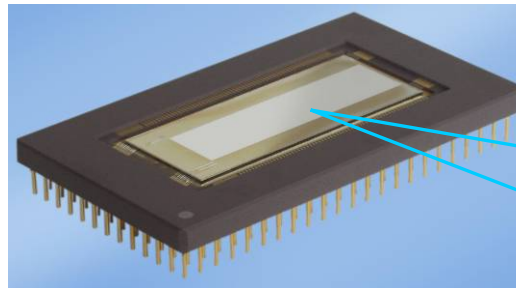
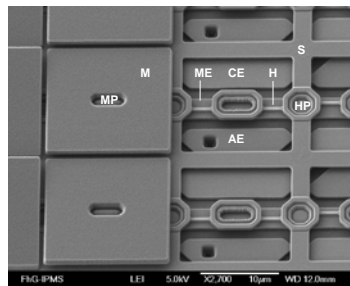
## ■ Piston mirror array

■ 48k

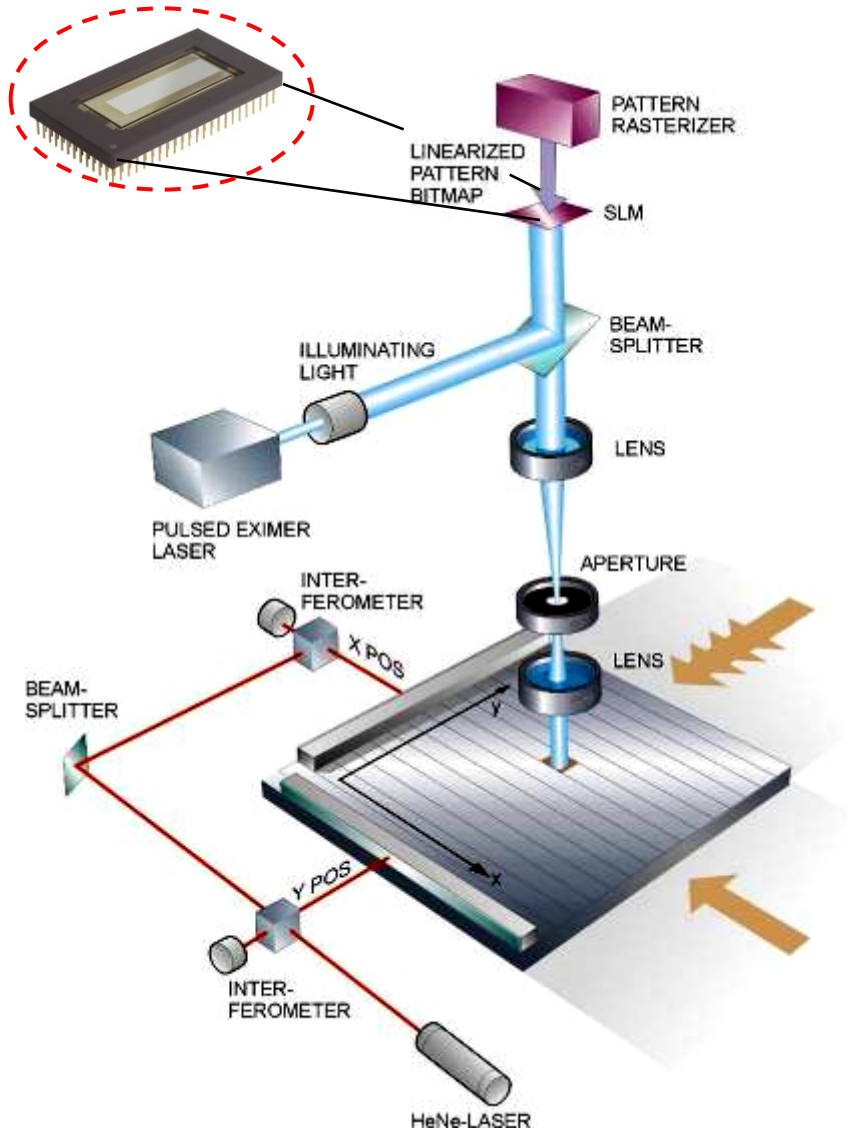


## ■ Single axis tilting mirror array

■ 1 M



# Laser Mask Writing: Operational Principle & Results



## Micronic Sigma7500

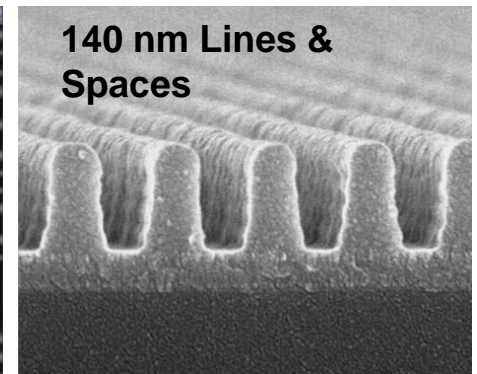
SLM-based semiconductor mask writer



MICRONIC MYDATA

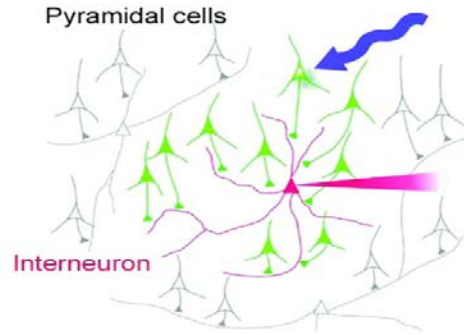
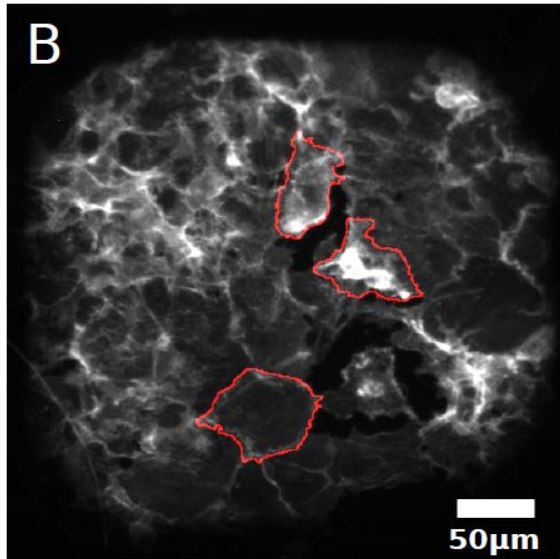


Pattern in resist

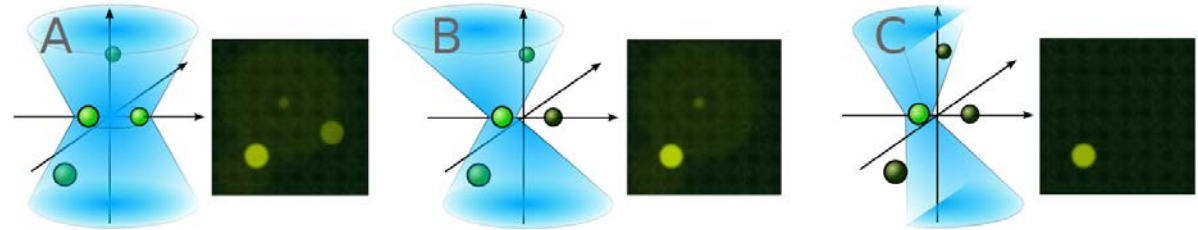
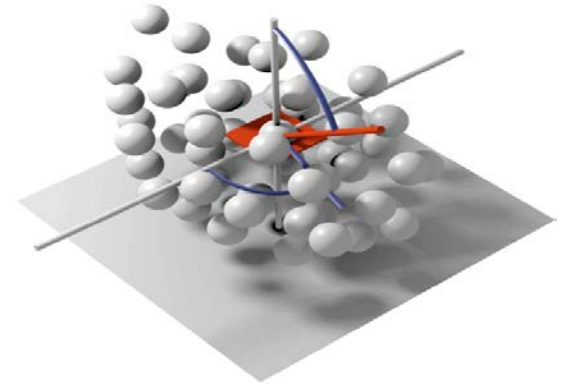


# Optogenetics: Operational Principle & Results

Controlled neuron excitation and gene activity



Macunso et al., Experimental Physiology, 2010



Application of double-MMA for structured microscope illumination

**Feedback System**

Take image of sample.  
Use of gratings allows sectioning.

Image processing

Illumination control

Widefield detection  
Image reconstruction

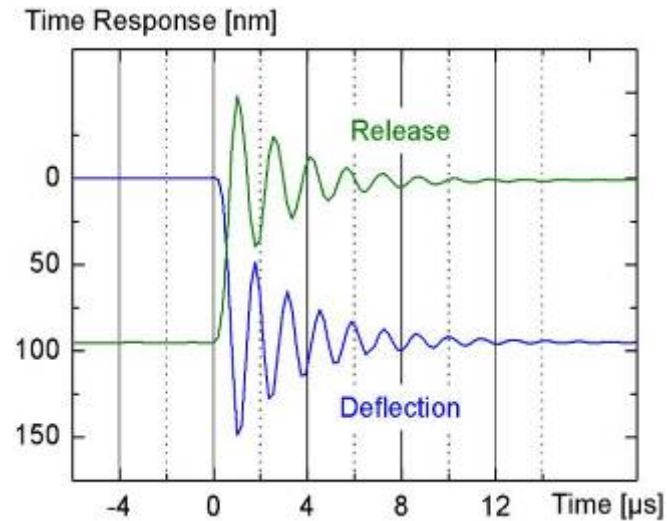
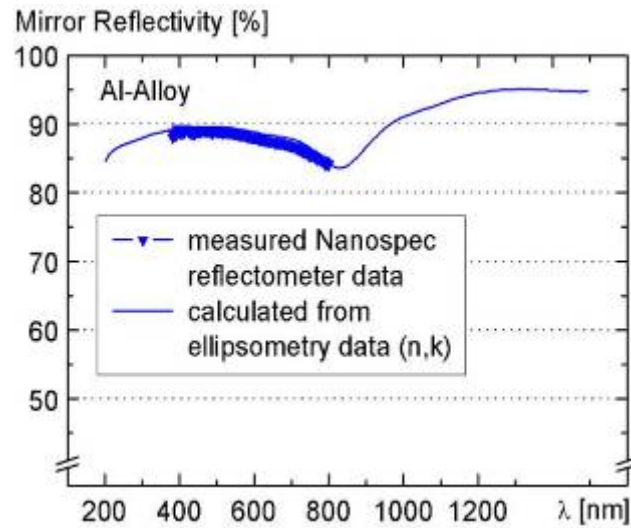
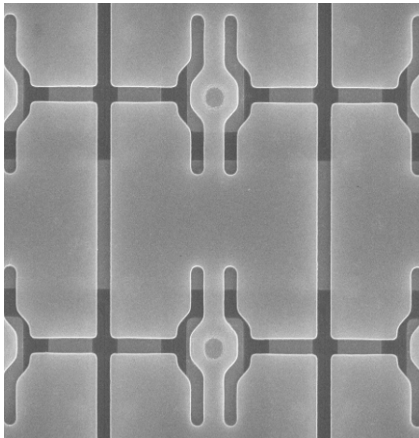
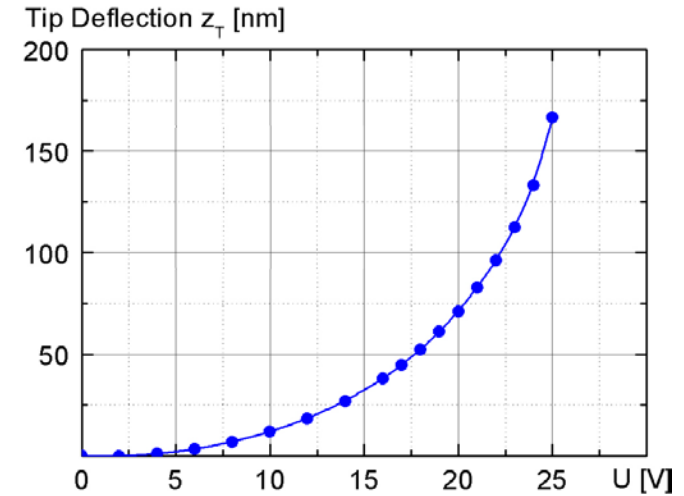
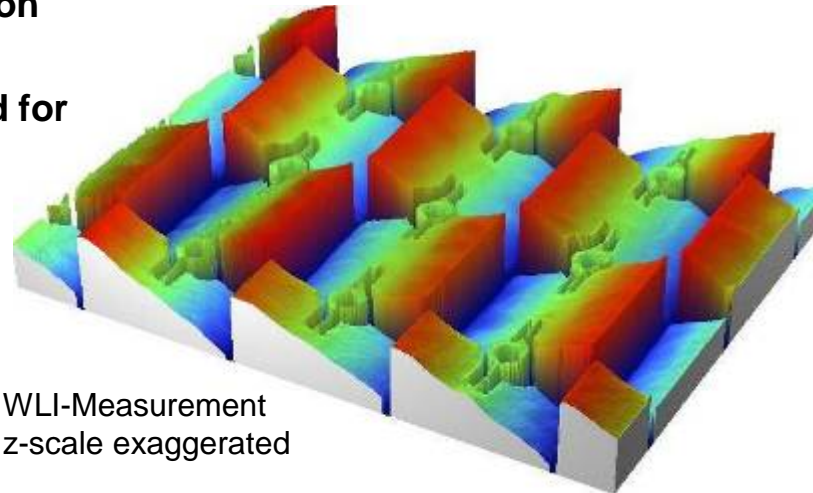
FIG-IPMS LEI 5.0kV X2,700 10µm WD 12.0mm



# Example 1: Spot-characterization of diffractive micro-mirror arrays

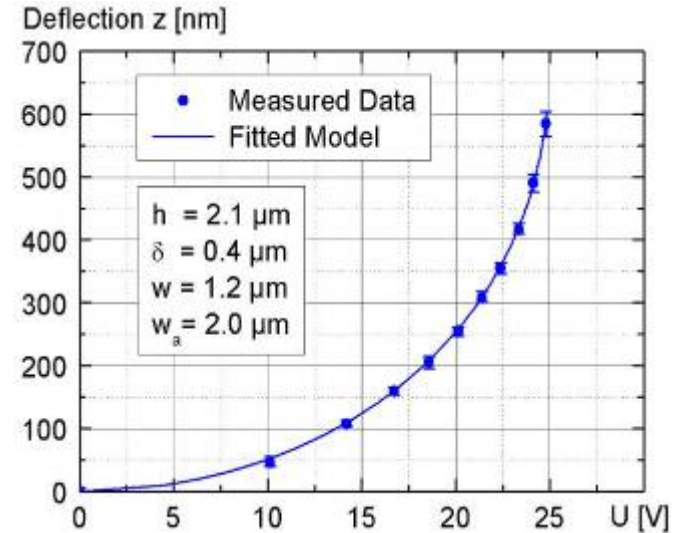
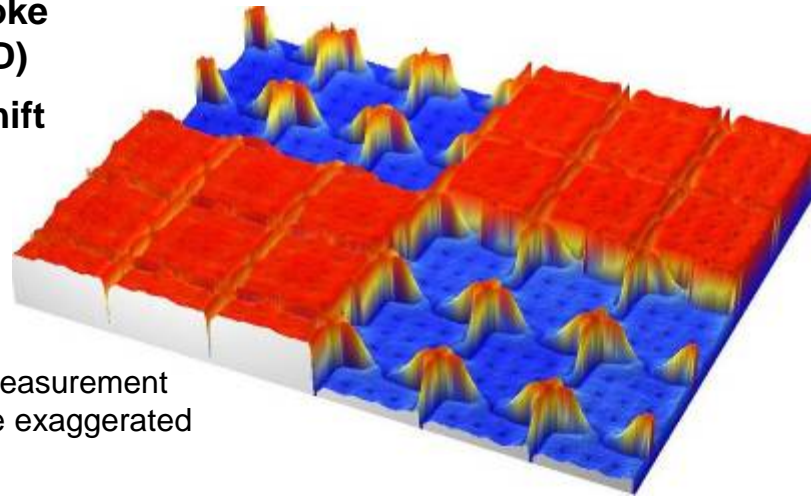
# Characteristics of 16 $\mu\text{m}$ Tilt-Mirrors

- Tip deflection  $> 150 \text{ nm}$
- $\lambda/4$  required for max. image contrast

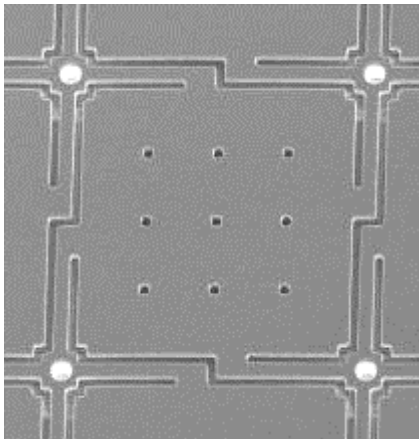


# Characteristics of 40 $\mu\text{m}$ Piston-Mirrors (1-Level Design)

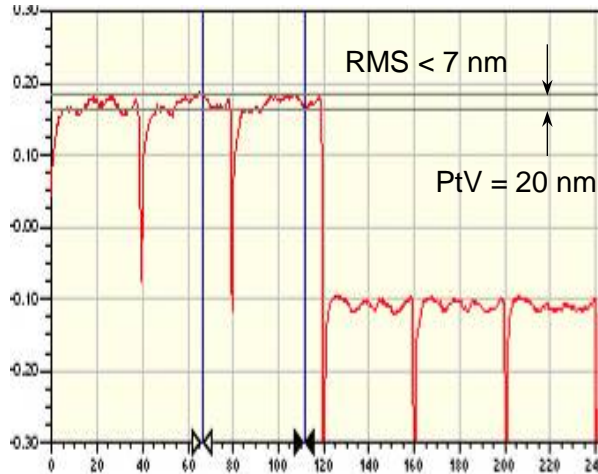
- 500 nm stroke (1.0  $\mu\text{m}$  OPD)
- $2\pi$  phase shift in the VIS



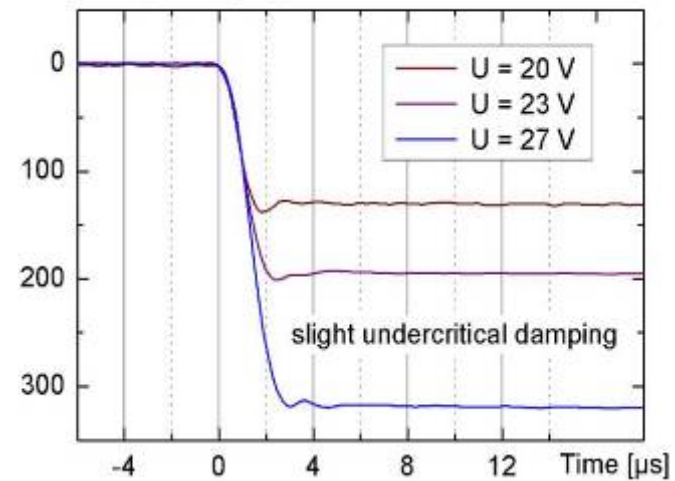
Mirror SEM



Mirror Planarity

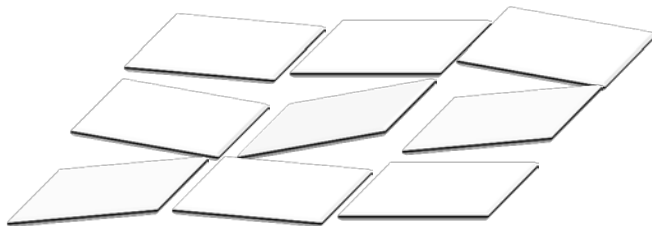


Time Response [nm]

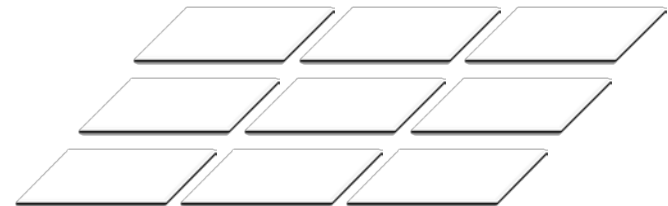


## Example 2: Calibration of diffractive micro-mirror arrays

■ MMA profile:

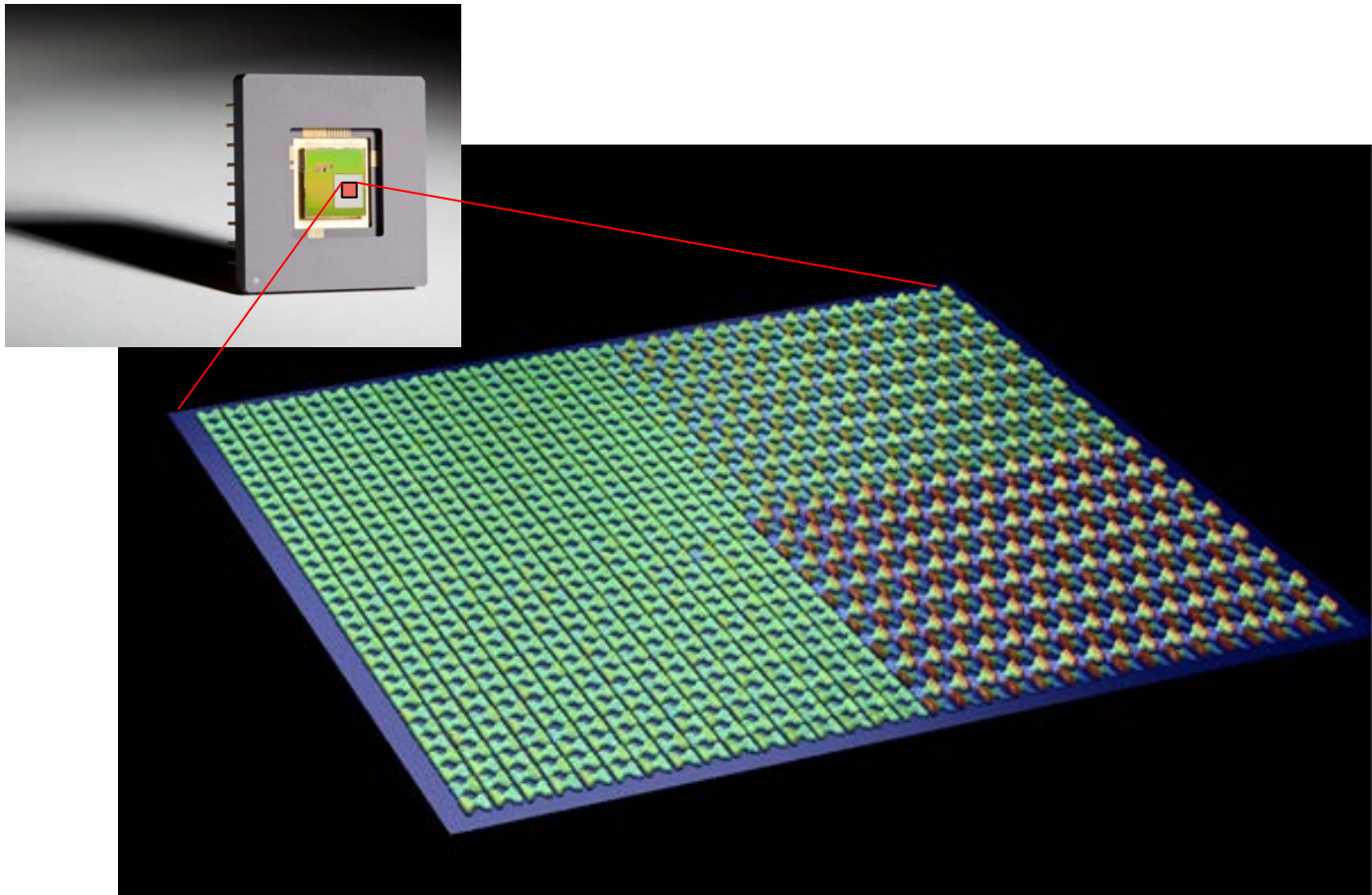


■ Desired state:



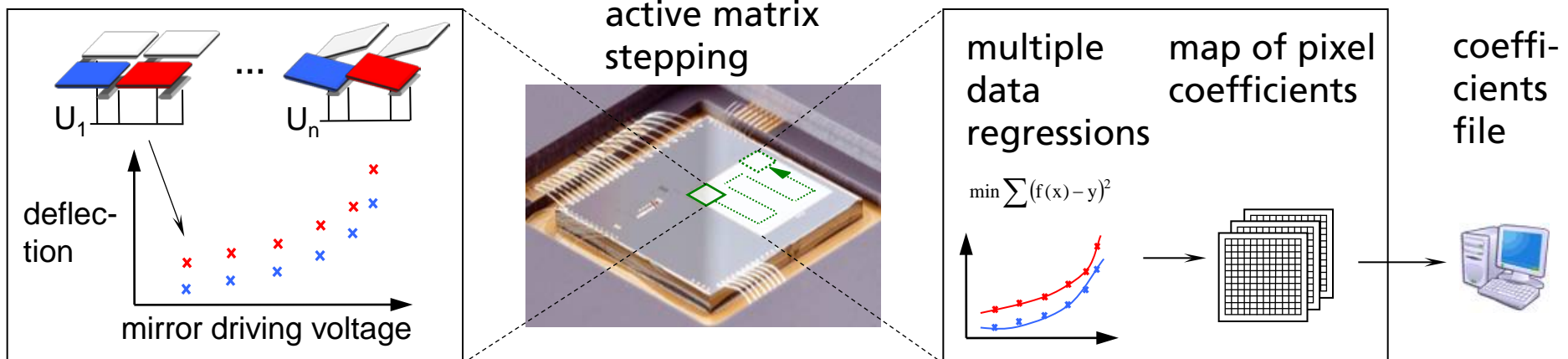
# Optical analysis of *micro- and nanostructures*

- How to measure a complete array of 64526 micromirrors with sub-nanometer z-resolution?



# Algorithm for single pixel MMA correction

1. Determination of micromirror's voltage-deflection response curves with a profilometric measurement system based on interferometry
2. Stepping of active MEMS area (>60.000 single mirrors)
3. Multiple data regressions to generate continuous response curves
4. Storage of coefficients

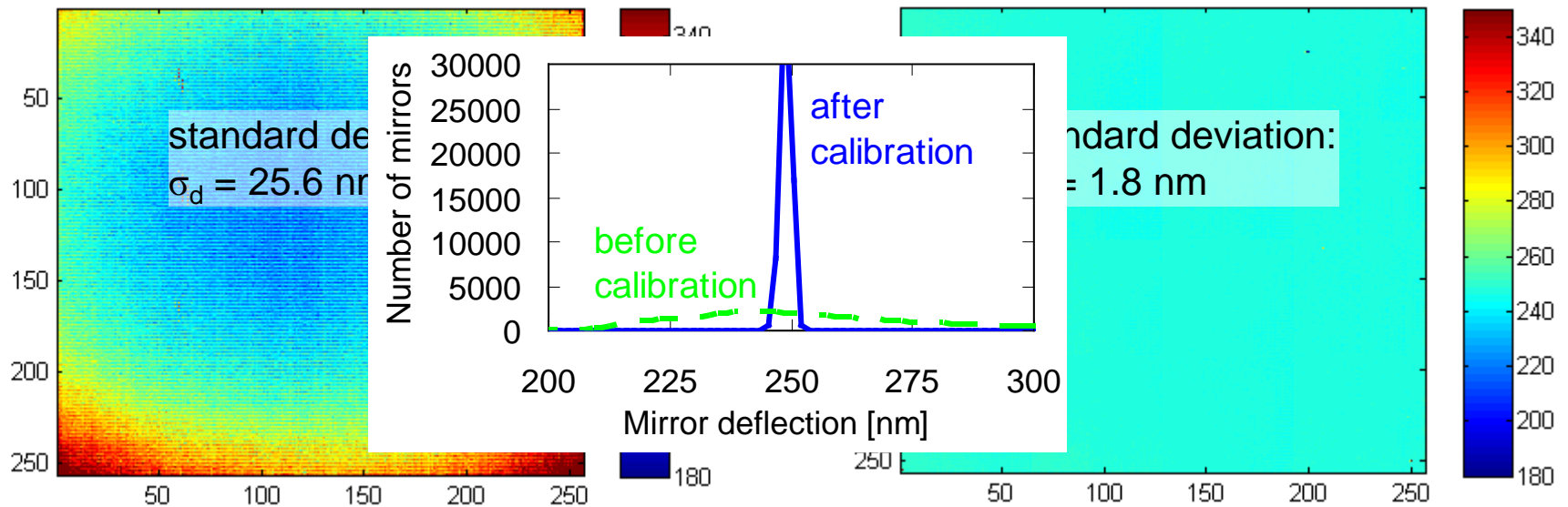


Source: D. Berndt, Proc. SPIE 8191 819100-1

# Calibration results – deflection homogeneity

*Micromirror mapping - target deflection 250 nm*

- MMA deflection without calibration
- Calibrated MMA deflection

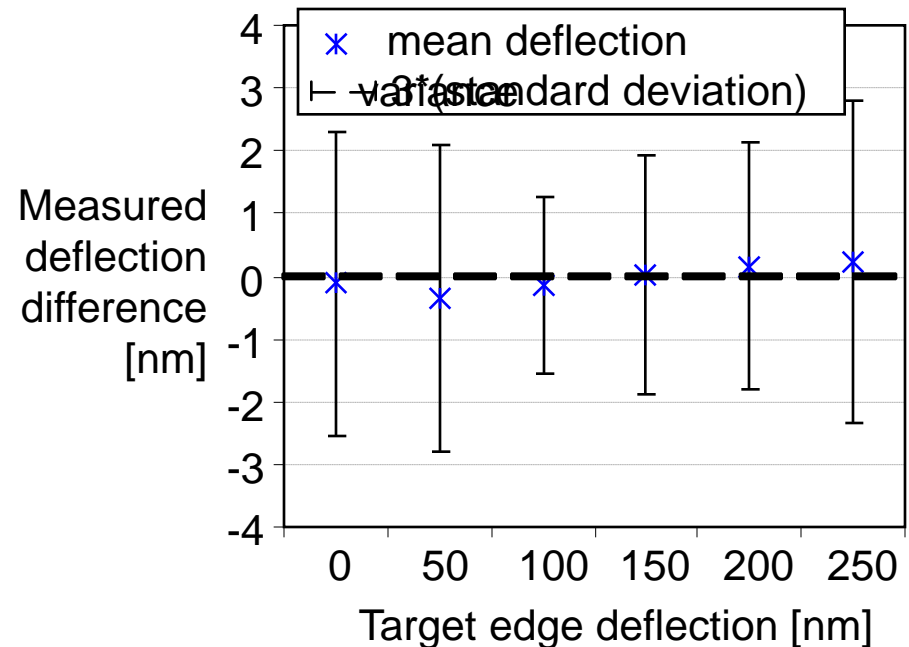
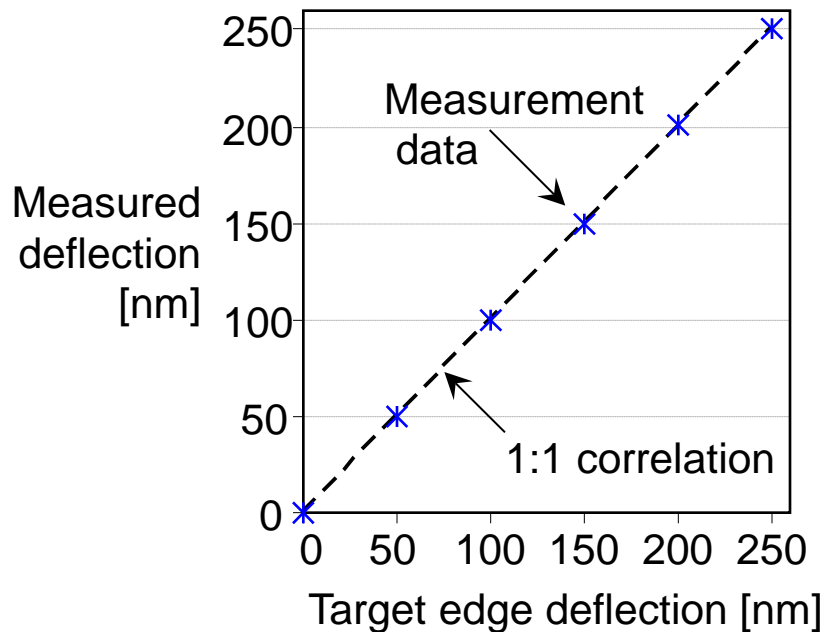


→ Decrease of deflection spread by more than a factor of 10

Source: D. Berndt, Proc. SPIE 8191 819100-1

# Calibration results – deflection accuracy

→ WLI resolution determines measured deflections:



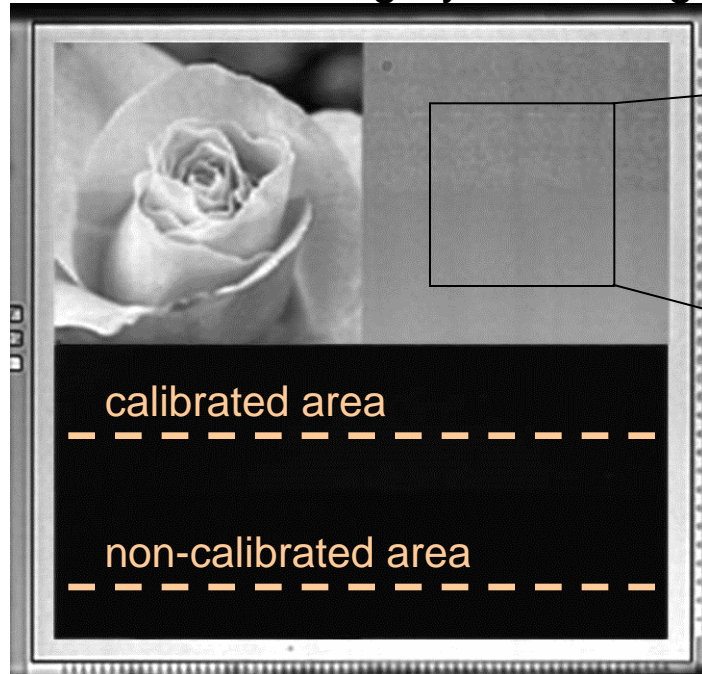
→ Accuracy of voltage-deflection response better than  $\lambda/100$

Source: D. Berndt, Proc. SPIE 8191 819100-1

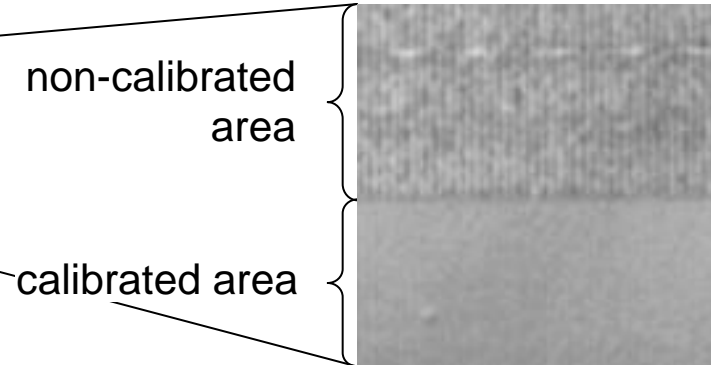


# Calibration results – Optical effects

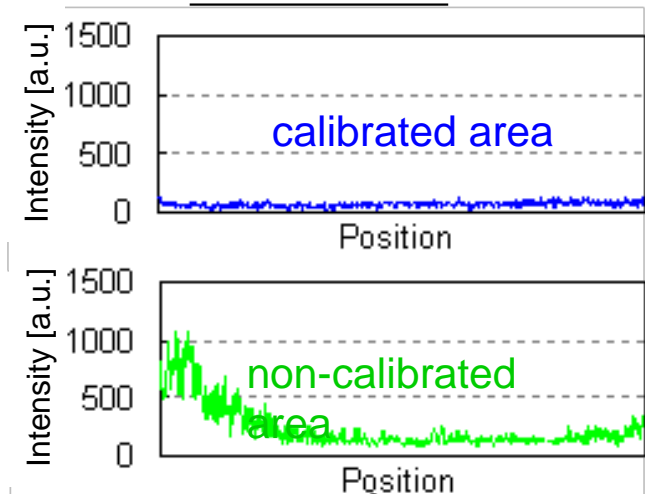
MMA modulated grayscale image



Magnified gray area



Cross section



- Contrast >1000, Homogeneity ~ 1 %
- WLI inspection with robust industrial system (~ hours of measurement) !

Source: D. Berndt, Proc. SPIE 8191 819100-1

## **Example 3: Analysis of wafer structures for SC manufacturing – „Vias and Trenches“**

- “Through Silicon Via (TSV)” E. Novak, 2010, Veeco

# Analysis of Vias (and Trenches) for SC-M

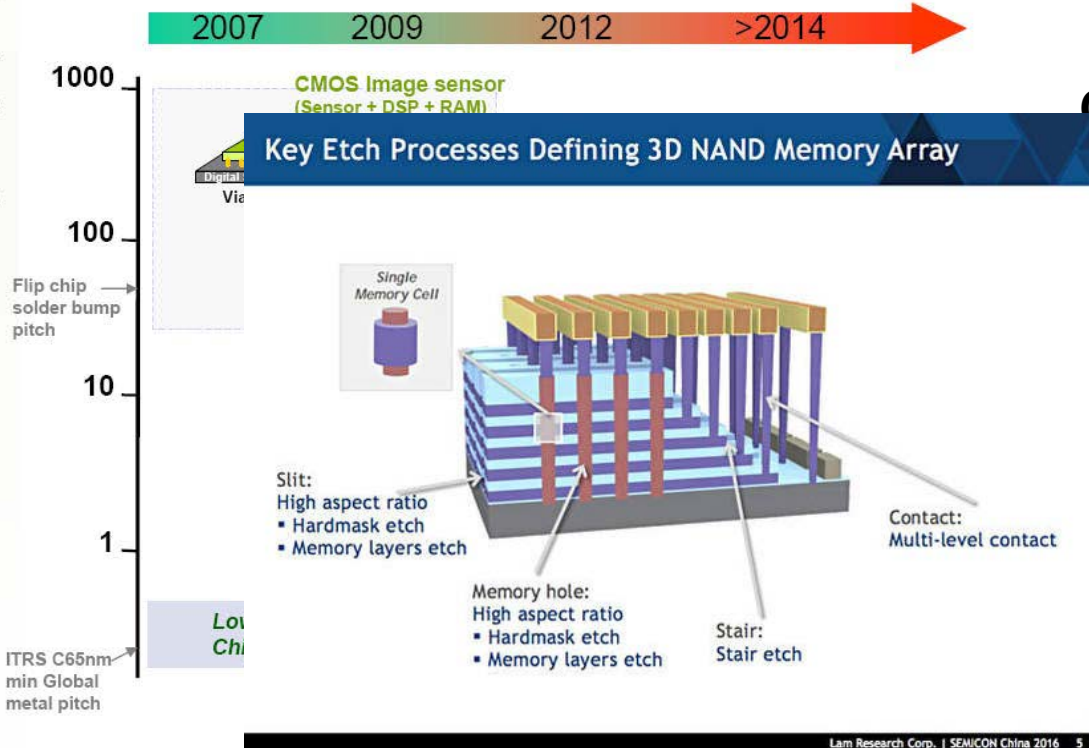
## ■ Via structures and SC development



### Applications of 3D integration



Vertical interconnect minimum pitch (μm)



### Characteristics

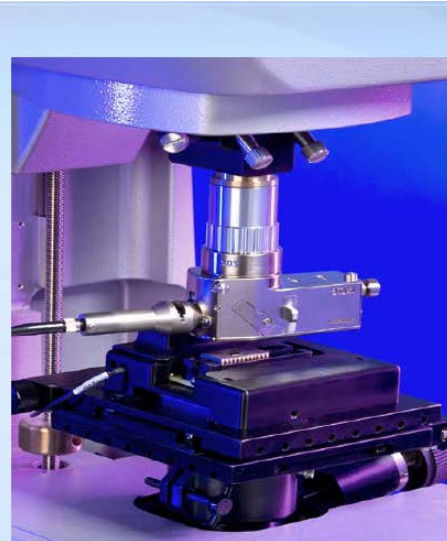
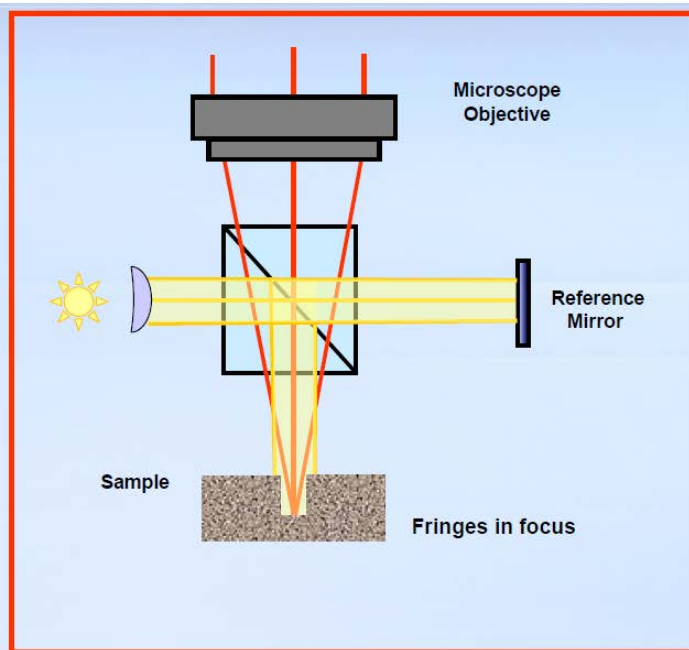
Size:  
2 μm lateral  
>10 μm vert.

„high aspect-ratio“  
~ 1: > 5 ...

Patrick Leduc - Conference on Frontiers of Characterization and Metrology for Nanoelectronics; March 27-29, 2007 | 9

# Analysis of Vias (and Trenches) for SC-M

- Experimental challenge: how to image a profile with “high aspect ratio”?



## WLI specifics:

- Use of (partial) coherent imaging
- Advanced data processing

Advantages of illumination from below of the objective

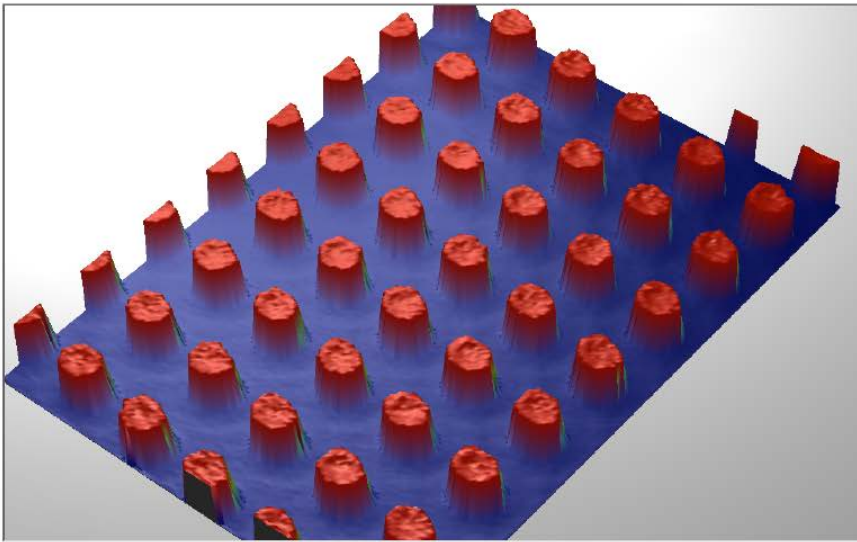
- Collimated illuminating beam better penetrates the via
- High numerical aperture of objective captures most light

# Analysis of Vias (and Trenches) for SC-M

## ■ Results of WLI tests:

### 3-Dimensional Interactive Display

Date:  
Time:

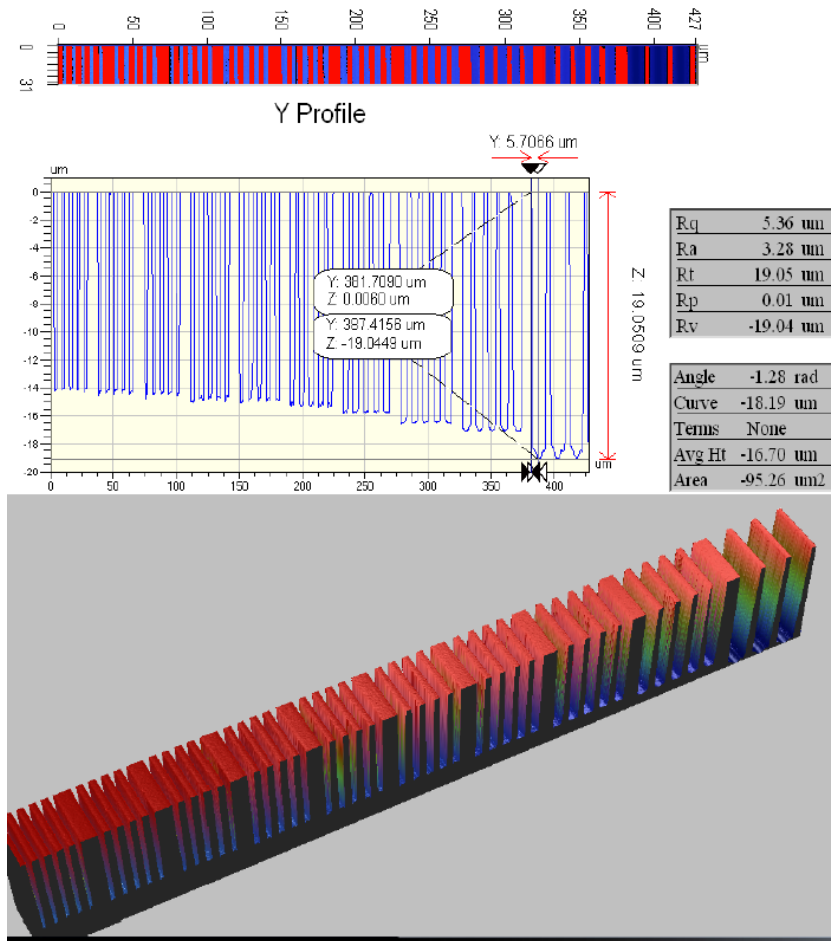


- 10 measurements, no remove/replace
- 3 micron vias:
  - Average Depth: 34.63  $\mu\text{m}$
  - Average width: 3.4  $\mu\text{m}$
- Data is shown inverted for clarity

- Via analysis starting at 1,5 $\mu\text{m}$  diameter amenable
- Aspect ratio 1 : 10...15

# Analysis of Vias (and Trenches) for SC-M

## ■ Results of WLI tests:



- Integrated image processing automatically identifies and reports individual trench data
- Average Depth: 14.3 microns (across all the lines)
- Width from 1 to 10 microns
- Average 1 Sigma Standard Deviation of depth: 70nm

- Trench analysis starting at 2 μm „line width“
- Aspect ratio 1: 20...40

# Summary - White Light Interferometry (WLI)

- WLI is an optical method measuring the change in phase of light.
- By means of numerical analysis, topography properties of micro and nanostructures can be indirectly determined - without user interaction.
- Advantages
  - Precise determination of structure properties
    - $< 1\text{nm}$  (z-resolution) with  $>100\mu\text{m}$  dynamic range
  - MEMS properties like micromirror deflection, cantilever mobility, micromechanical stability become amenable
  - Access to optical constants & thickness of *structured* thin films
  - Non-destructive, fast
- Typical application:
  - Combination with microscopy ( $< 1\ \mu\text{m}$  lateral resolution)
  - Time resolved analysis (stationary,  $< 100\ \text{ns}$  resolution)

# CONCLUSION



## Ellipsometry, X-ray Reflectometry, Interferometry

- Photons are a versatile tool for the non-destructive analysis of micro and nanostructures even at sub-nanometer scales
- The combination of high resolution capabilities together with spectral- and time-resolved information steadily extends the industrial application range

# Thank you for your attention!